

## Transepithelial $\text{Na}^+$ Transport and the Intracellular Fluids: A Computer Study

Mortimer M. Civan and Richard J. Bookman

Departments of Physiology and Medicine, University of Pennsylvania School of Medicine, Philadelphia, Pennsylvania 19104

**Summary.** Computer simulations of tight epithelia under three experimental conditions have been carried out, using the rheogenic nonlinear model of Lew, Ferreira and Moura (*Proc. Roy. Soc. London. B* **206**:53–83, 1979) based largely on the formulation of Koefoed-Johnsen and Ussing (*Acta Physiol. Scand.* **42**:298–308, 1958). First, analysis of the transition between the short-circuited and open-circuited states has indicated that (i) apical  $\text{Cl}^-$  permeability is a critical parameter requiring experimental definition in order to analyze cell volume regulation, and (ii) contrary to certain experimental reports, intracellular  $\text{Na}^+$  concentration ( $c_{\text{Na}}^i$ ) is expected to be a strong function of transepithelial clamping voltage. Second, analysis of the effects of lowering serosal  $\text{K}^+$  concentration ( $c_{\text{K}}^o$ ) indicates that the basic model cannot simulate several well-documented observations; these defects can be overcome, at least qualitatively, by modifying the model to take account of the negative feedback interaction likely to exist between the apical  $\text{Na}^+$  permeability and  $c_{\text{Na}}^i$ . Third, analysis of the effects induced by lowering mucosal  $\text{Na}^+$  concentration ( $c_{\text{Na}}^o$ ) strongly supports the concept that osmotically induced permeability changes in the apical intercellular junctions play a physiological role in conserving the body's stores of  $\text{NaCl}$ . The analyses also demonstrate that the importance of  $\text{Na}^+$  entry across the basolateral membrane is strongly dependent upon transepithelial potential,  $c_{\text{Na}}^o$  and  $c_{\text{K}}^o$ ; under certain conditions, net  $\text{Na}^+$  entry could be appreciably greater across the basolateral than across the apical membrane.

**Key words** sodium transport · cell volume · intracellular fluids · paracellular pathway · tight epithelia · serosal potassium · nonlinear models

### Introduction

In recent years, an enormous volume of information has been published concerning transepithelial transport of solutes and water. Data are being obtained not only by a variety of black box approaches (Ussing, 1960; Leaf, 1965; Lindemann, 1980), but increasingly by application of element-specific biophysical techniques (Civan, 1978; Gupta & Hall, 1979; Bond, Shporer, Peterson & Civan, *in press*). Clearly, some sort of formalism is necessary in order to: (i) correlate results from different sources, (ii) examine critically whether current concepts suffice

to account for the data, (iii) test the plausibility of new concepts, and (iv) help identify critical pieces of information not yet available, but essential for our understanding of transport physiology.

The limitations of the traditional linear formalisms in wide use have long been recognized. The equivalent circuit approach has been utilized with notable success (Hodgkin & Huxley, 1952); however, Finkelstein and Mauro (1963) have pointed out that in its most commonly used form, the equivalent circuit is an inappropriate vehicle for simulating transient electrical phenomena. Linear equilibrium thermodynamics has also been of value in analyzing transport phenomena (Essig & Caplan, 1979). However, its theoretical development rests on at least three assumptions (Katchalsky & Curran, 1967) which are true for systems close to equilibrium, and which may or may not be true for systems far from equilibrium (Rothschild, Elias, Essig & Stanley, 1980; Essig & Caplan, 1981). Calculated from published values for a wide spectrum of tissues (Handler, Preston & Orloff, 1969; Guynn & Veech, 1973; Erecinska, Wilson & Nishiki, 1978), the extramitochondrial phosphorylation potential (Klingenberg, 1968; Slater, 1969) can be estimated to be  $\geq 11$ – $13 \text{ kcal mol}^{-1}$ ; these values are far greater than the molar thermal energy, suggesting (but not proving) that epithelia operate far from equilibrium. These considerations do not preclude the possibility of utilizing linear formalisms to great advantage. However, the theoretical basis for their applicability remains uncertain.

In view of the uncertainties and limitations of current linear formalisms, we have turned to nonlinear alternatives. Specifically, several promising models (Hviid Larsen, 1978; Hviid Larsen & Kristensen, 1978; Thomas & Mikulecky, 1978; Lew, Ferreira & Moura, 1979) applicable to transepithelial transport have recently been developed. In the pres-

ent study, we have utilized the basic model of Lew et al. (1979) because their formulation both permits analysis of transient phenomena and has already been demonstrably helpful in clarifying our understanding of transepithelial transport of sodium. The present work constitutes an extension of that model in analyzing three experimental problems with which this laboratory has been concerned: (i) the changes in intracellular composition accompanying the transition from the short-circuited to the open-circuited state, (ii) the intracellular events associated with initially removing and then restoring potassium to the serosal medium bathing toad urinary bladder and frog skin, and (iii) the physiologic role of the intercellular limiting or tight junctions in regulating transepithelial sodium transport.

It must be stressed that the present work does *not* constitute an effort to develop a model readily accommodating all published observations. Rather, the strategy adopted by Lew et al. (1979) has been retained. The model used consists of a minimal number of constructs, almost all of which are widely accepted. No modification is incorporated until the basic model is clearly demonstrated to be incapable of simulating well-documented observations. We anticipate that the model will undergo an increasing number of modifications as it is applied to other experimental problems.

## Materials and Methods

### General Description of Model

The model developed by Lew et al. (1979) for transport of Na<sup>+</sup> primarily across tight epithelia is based largely upon the formulation of Koefoed-Johnsen and Ussing (1958). A three-compartment system is considered, consisting of perfectly stirred, homogeneous mucosal (*m*), serosal (*s*) and intracellular (*c*) phases. The three compartments (here identified by the index *k*) are separated by three permeability barriers (identified by the index *j*): the apical plasma membrane (*a*), the basolateral membrane (*bl*) and the apical limiting or tight junctions (*jcn*). Intracellular binding and compartmentalization of solutes are thought to be negligible. Only three ions (identified by the index *i*) are considered to cross the permeability barriers at significant rates: Na<sup>+</sup>, K<sup>+</sup>, and Cl<sup>-</sup>; a polyanion (*X<sup>z+</sup>*) is constrained to the intracellular compartment, and water is considered to be at equilibrium across the basolateral membrane. Solvent drag and unstirred aqueous layers are neglected.

Lew et al. (1979) considered ionic fluxes to cross each of the permeability barriers by electrodiffusion and by specialized transfer processes. In their basic model, the only specialized transport mechanism was the Na/K-exchange pump at the basolateral membrane. To a limited extent, they also considered possible movement of Cl<sup>-</sup> across the apical plasma membrane, both by a chloride pump and by electroneutral entry of NaCl. Because of the incomplete information currently available concerning these putative specialized transfer pathways in toad bladder and frog skin, we have limited consideration of specialized chloride transfer to an examination of a chloride pump. The electrodiffusive

component of each ionic flux is presumed to conform to a constant field expression (Goldman, 1943; Hodgkin & Katz, 1949).

In their initial published model, Lew et al. (1979) treated the Na/K-exchange pump as a current source characterized by three identical noncooperative sites at the inner surface, and two identical noncooperative sites at the outer surface of the basolateral membrane (Hoffman & Tosteson, 1971; Garay & Garrahan, 1973). The apparent dissociation constants of the inner and outer sites were taken to be constant. More, recently, the model has been modified (Lew, *private communication*) to take account of the observation that these apparent dissociation constants on the intracellular and serosal surfaces appear to be influenced by the intracellular K<sup>+</sup> concentration (*c<sub>K</sub><sup>s</sup>*) and the serosal Na<sup>+</sup> concentration (*c<sub>Na</sub><sup>s</sup>*), respectively (Garay & Garrahan, 1973). This latter approach has been adopted here. The stoichiometry (*r*) of the pump was considered to be 3Na<sup>+</sup> outwards for 2K<sup>+</sup> inwards.

In the basic model Lew et al. (1979) assumed that hydrostatic pressure differences were negligible and that all activity and reflection coefficients were equal to one. Furthermore, in general, the permeabilities (*P<sub>j</sub><sup>i</sup>*) of all ions (*i*) at all permeability barriers (*j*) were presumed constant during the course of any given experiment. The sole exception was the apical Na<sup>+</sup> permeability (*P<sub>a</sub><sup>Na</sup>*), which was expressed as the inverse function of mucosal Na<sup>+</sup> concentration (*c<sub>Na</sub><sup>m</sup>*), suggested by Fuchs, Hviid Larsen and Lindemann (1977).

The current treatment of the basic model differs in only two respects. First, account has been taken of the apparent inverse relationship between (*P<sub>a</sub><sup>Na</sup>*) and intracellular Na<sup>+</sup> concentration (*c<sub>Na</sub><sup>c</sup>*) (Erlj & Smith, 1973; Leblanc & Morel, 1975; Morel & Leblanc, 1975; Lewis, Eaton & Diamond, 1976; Cuthbert & Shum, 1977; Turnheim, Frizzell & Schultz, 1978; Weinstein, Rosowski, Peterson, Delalic & Civan, 1980). Second, the reflection coefficient (*σ<sub>KCl</sub>*) for KCl at the basolateral membrane has been permitted to assume values other than one (Hviid Larsen, 1978; Hviid Larsen & Kristensen, 1978). Unless otherwise specified, values chosen for all constants have been taken to be those of Lew et al. (1979) to facilitate comparison with their model.

### Definition of Terms

The following list provides a glossary of the symbols used in the manuscript. In parentheses are entered the units and, where appropriate, the values used.

$c_i^k$	concentration of <i>i</i> th ion in <i>k</i> th compartment (mM) (unless otherwise stated, the Na <sup>+</sup> , Cl <sup>-</sup> and K <sup>+</sup> concentrations of both bathing media were 120, 122.5 and 2.5 mM, respectively)
$E^j$	difference in electrical potential across <i>j</i> th permeability barrier: <i>j</i> = <i>a</i> , mucosal relative to intracellular potential; <i>j</i> = <i>bl</i> , intracellular relative to serosal potential; <i>j</i> = <i>jcn</i> , mucosal relative to serosal potential (mV)
$F$	Faraday constant (96,484 cou equiv <sup>-1</sup> )
$f$	dimensionless factor expressing inverse dependence of mucosal Na <sup>+</sup> permeability upon intracellular Na <sup>+</sup> concentration
$f_{\min}$	minimum permissible value for <i>f</i>
$g_i^j$	partial conductance of <i>i</i> th ion at <i>j</i> th barrier (μS cm <sup>-2</sup> )
$G_a^s$	total conductance of apical membrane (μS cm <sup>-2</sup> )
$G_{bl}^s$	total conductance of basolateral membrane (μS cm <sup>-2</sup> )
$G_{\Sigma}^{\text{cell}}$	total conductance of transcellular transepithelial pathway (μS cm <sup>-2</sup> )
$G_j^j$	total conductance of <i>j</i> th permeability barrier (μS cm <sup>-2</sup> )
$G_{\Sigma}^{\text{jcn}}$	total conductance of intercellular limiting or tight junctions (μS cm <sup>-2</sup> )
$G_T$	total tissue conductance (μS cm <sup>-2</sup> )
$I_{\Sigma}^a$	total current across apical membrane (μA cm <sup>-2</sup> )

$I_{Na}^{bl}$	total current across basolateral membrane ( $\mu A\ cm^{-2}$ )
$(I_{Na}^{bl})_{ed}$	electrodiffusive component of total Na <sup>+</sup> current across the basolateral membrane ( $\mu A\ cm^{-2}$ )
$(I_{Na})_T$	total net transepithelial Na <sup>+</sup> current from mucosa to serosa ( $\mu A\ cm^{-2}$ )
$I_z^{cell}$	total current flow through transcellular transepithelial pathway ( $\mu A\ cm^{-2}$ )
$I_i^j$	current carried by <i>i</i> th ion across <i>j</i> th permeability barrier ( $\mu A\ cm^{-2}$ )
$I_z^{icn}$	total current across intercellular limiting junctions ( $\mu A\ cm^{-2}$ )
$I_T$	total transepithelial current ( $\mu A\ cm^{-2}$ )
<i>i</i>	subscript index referring to one of 4 ions: Na <sup>+</sup> , Cl <sup>-</sup> , K <sup>+</sup> , X <sup>z<sub>x</sub></sup>
<i>j</i>	superscript referring to one of 3 permeability barriers: (a) apical membrane, (bl) basolateral membrane, and (jcn) intercellular tight junction
<i>k, k+1</i>	superscripts referring to the two fluid compartments adjoining the <i>j</i> th barrier: ( <i>j=a</i> ) <i>k</i> =mucosal medium ( <i>m</i> ), and <i>k+1</i> =intracellular fluid ( <i>c</i> ); ( <i>j=bl</i> ) <i>k</i> =c, and <i>k+1</i> =serosal medium ( <i>s</i> ); ( <i>j=jcn</i> ) <i>k</i> =m, and <i>k+1</i> =s
$(K_{Cl})_p$	apparent dissociation constant of the Cl-site complex for the Cl <sup>-</sup> pump at the apical membrane (2 mM)
$(K_K^{bl})$	apparent dissociation constant of the K-site complex for the Na/K-activated pump at the serosal surface of the basolateral membrane
$(K_{Na}^{bl})$	apparent dissociation constant of the Na-site complex for the Na/K-exchange pump at the intracellular surface of the basolateral membrane
$n_i^c$	intracellular content of Na <sup>+</sup> , K <sup>+</sup> , Cl <sup>-</sup> , or indiffusible polyanion X <sup>z<sub>x</sub></sup> (mmol cm <sup>-2</sup> )
$P_i^j$	permeability of the <i>i</i> th ion at the <i>j</i> th permeability barrier (cm sec <sup>-1</sup> )
$P_{Cl}^a$	apical Cl <sup>-</sup> permeability ( $5.0 \times 10^{-8}$ cm sec <sup>-1</sup> )
$P_K^a$	apical K <sup>+</sup> permeability ( $1.0 \times 10^{-7}$ cm sec <sup>-1</sup> )
$P_{Cl}^{bl}$	basolateral Cl <sup>-</sup> permeability ( $1.8 \times 10^{-7}$ cm sec <sup>-1</sup> )
$P_{Na}^{bl}$	basolateral Na <sup>+</sup> permeability ( $7.3 \times 10^{-8}$ cm sec <sup>-1</sup> )
$P_{Cl}^{jcn}$	junctional Cl <sup>-</sup> permeability ( $2.5 \times 10^{-7}$ cm sec <sup>-1</sup> )
$P_K^{jcn}$	junctional K <sup>+</sup> permeability ( $7.0 \times 10^{-8}$ cm sec <sup>-1</sup> )
$P_{Na}^{jcn}$	junctional Na <sup>+</sup> permeability ( $5.0 \times 10^{-8}$ cm sec <sup>-1</sup> )
<i>p</i>	subscript referring to a pump transport mechanism
<i>R</i>	perfect gas constant [8.31434 joules mol <sup>-1</sup> · (degree Kelvin) <sup>-1</sup> ]
<i>r</i>	ratio of the rate of Na <sup>+</sup> efflux to that of K <sup>+</sup> influx into the cell through the Na/K-exchange pump (1.5)
<i>T</i>	absolute temperature (293.2 °K)
$V^j$	$E^j[(zF)/(RT)]$ (dimensionless)
$v^c$	intracellular volume (cm <sup>3</sup> · cm <sup>-2</sup> )
<i>X</i>	indiffusible polyanions within the intracellular compartment
<i>z<sub>i</sub></i>	valence of the <i>i</i> th ion (equiv mol <sup>-1</sup> )
<i>z<sub>x</sub></i>	mean valence of the intracellular anions X
$\pi^m$	osmolality of the mucosal medium [mOsm · (kg water) <sup>-1</sup> ]
$\sigma_{KCl}$	reflection coefficient for KCl at the basolateral membrane (taken to be either 1.00 or 0.95)
$(\phi_i^j)$	flux of the <i>i</i> th ion through a specialized transport mechanism at the <i>j</i> th permeability barrier ( $\mu mol\ cm^{-2}\ sec^{-1}$ )
$(\phi_i^j)_{max}$	maximal rate of net transport of the <i>i</i> th ion through a specialized transport mechanism at the <i>j</i> th permeability barrier ( $\mu mol\ cm^{-2}\ sec^{-1}$ )

### Presentation of Equations Used

$$I_i^j = P_i^j F V^j \left[ \frac{c_i^k - c_i^{k+1} e^{-z_i V^j}}{1 - e^{-z_i V^j}} \right] + z_i F \phi_i^j, \quad V \neq 0 \quad (1)$$

$$I_i^j = P_i^j F (c_i^k - c_i^{k+1}) + z_i F \phi_i^j, \quad V = 0 \quad (2)$$

$$P_{Na}^a = (P_{Na}^a)_{max} \left( \frac{30}{30 + c_{Na}^m} \right) f \quad (3)$$

$$f = \left( 1 - \frac{c_{Na}^c}{50} \right) \left( \frac{5}{3} \right), \quad \text{where } f \geq f_{min} > 0 \quad (4)$$

$$\phi_{Na}^a = \phi_{Cl}^{bl} = \phi_K^a = 0 \quad (5)$$

$$\phi_{Na}^{bl} = (\phi_{Na}^{bl})_{max} \left[ \frac{c_{Na}^c}{c_{Na}^c + K_{Na}^{bl}} \right]^3 \left[ \frac{c_K^s}{c_K^s + K_K^{bl}} \right]^2 \quad (6)$$

$$K_{Na}^{bl} = 0.2 \left( 1 + \frac{c_K^c}{8.33} \right) \quad (7)$$

$$K_K^{bl} = 0.1 \left( 1 + \frac{c_{Na}^s}{18.5} \right) \quad (8)$$

$$\phi_K^{bl} = -\phi_{Na}^s/r \quad (9)$$

$$(\phi_{Cl}^a)_p = (\phi_{Cl}^a)_{p,max} \left[ \frac{c_{Cl}^m}{c_{Cl}^m + (K_{Cl}^a)_p} \right] \quad (10)$$

$$c_{Na}^k + c_K^k = c_{Cl}^k + c_x^k z_x^k \quad (11)$$

$$\begin{aligned} (1/v^c) [n_K^c + n_{Cl}^c (2\sigma_{KCl} - 1) + n_{Na}^c + n_x^c] \\ = c_K^s (2\sigma_{KCl} - 1) + c_{Cl}^s + c_{Na}^s \end{aligned} \quad (12)$$

$$I_z^a = I_z^{bl} \equiv I_z^{cell} \quad (13)$$

$$I_T = I_z^{cell} + I_z^{jcn} \quad (14)$$

$$\begin{aligned} g_i^j = \frac{P_i^j F^2}{RT(1 - e^{-z_i V^j})^2} \{ (c_i^k - c_i^{k+1} e^{-z_i V^j}) [1 - e^{-z_i V^j} (1 + z_i V^j)] \\ + z_i V^j c_i^{k+1} e^{-z_i V^j} (1 - e^{-z_i V^j}) \}, \quad V^j \neq 0 \end{aligned} \quad (15)$$

$$g_i^j = \frac{P_i^j F^2}{RT} \left( \frac{c_i^k + c_i^{k+1}}{2} \right), \quad V^j = 0 \quad (16)$$

$$G_z^j \equiv \sum_i g_i^j \quad (17)$$

$$G_T \equiv G_z^{cell} + G_z^{jcn} \quad (18)$$

$$G_z^{cell} = \left[ \frac{1}{G_z^a} + \frac{1}{G_z^{bl}} \right]^{-1} \quad (19)$$

### Comments on the Basic Equations

The first two equations state that the net current carried by the *i*th ion across the *j*th barrier is given by the sum of a constant field expression (first term, r.h.s.) and a contribution from any specialized transfer function within that barrier (second term, r.h.s.). Equation (3) expresses the inverse relationship between  $P_{Na}^a$  and  $c_{Na}^m$  reported by Fuchs et al. (1977) and incorporated in the model of Hviid Larsen and Kristensen (1978).

The factor (*f*) of Eq. (3) expresses the putative inverse relationship between  $P_{Na}^a$  and  $c_{Na}^c$ .

Equation (4) presents an empirical definition of (*f*). Other expressions could also be used; further data are needed to determine the most appropriate formulation. The merit of Eq. (4) is that it expresses the inverse relationship between  $P_{Na}^a$  and  $c_{Na}^c$  in particularly simple form. Because of the introduction of the factor (5/3), *f*=1 under baseline short-circuited conditions. The normalization of  $c_{Na}^c$  by the factor 50 has been suggested by electrometric (DeLong & Civan, 1978, 1979) and microprobe (Civan, Hall & Gupta, 1980) analyses of toad bladder. Incubation of this tissue with Ringer's solution nominally free of K<sup>+</sup> for ~1 hr reduces

transepithelial conductance severalfold and also lowers  $a_K^c$  (intracellular K<sup>+</sup> activity) by a mean value of approximately 30 mM (DeLong & Civan, 1978, 1979); however, this fall in conductance can be noted in some experiments at a time when  $a_K^c$  has fallen by only 20–25 mM. We approximate the intracellular activity coefficient for K<sup>+</sup> by 0.76, the value characterizing K<sup>+</sup> in the external medium. Thus, removal of external K<sup>+</sup> markedly reduces transepithelial conductance when  $c_K^c$  has fallen by some 30 mM. Electron microprobe analysis suggests that this fall in  $c_K^c$  is linked to a nearly equimolar gain in  $c_{Na}^c$ , in this case 30 mM. Insofar as the baseline value of  $c_{Na}^c$  is close to 20 mM in toad bladder (Rick, Dörge, Macknight, Leaf & Thureau, 1978b; Civan et al., 1980), ( $f$ ) is probably reduced to some minimal value  $f_{min}$  when  $c_{Na}^c$  rises to 50 mM. It is unlikely that  $f_{min}$  ever actually falls to zero following removal of serosal K<sup>+</sup>; Robinson and Macknight (1976b) have reported continued apical Na<sup>+</sup> entry under these conditions.

Equations (5)–(6) and (9)–(10) state that the only specialized transport processes to be considered in the present work are the Na/K-exchange pump at the basolateral membrane and a Cl<sup>−</sup> pump at the apical membrane. The form of Eq. (6) expresses both the concept of noninteraction between the inner and outer sites of the Na/K-exchange pump (Hoffman & Tosteson, 1971; Garay & Garrahan, 1973) and the stoichiometry of the pump. Equations (7)–(8) define the variable affinities of the Na<sup>+</sup> and K<sup>+</sup> binding sites on the intracellular and serosal surfaces, respectively, of the plasma membrane.

Electron microprobe measurements of intracellular chloride concentration in toad bladder (Rick et al., 1978b; Civan et al., 1980) and frog skin (Rick, Dörge, Arnim & Thureau, 1978a), electrometric determinations of intracellular chloride activity in frog skin (Nagel, Garcia-Diaz & Armstrong, *in press*), and intracellular measurements of membrane potential in frog skin (Nagel, 1976, 1980; Helman & Fisher, 1977; Helman, Nagel & Fisher, 1979; Nagel, Pope, Peterson & Civan, 1980) suggest that these tight epithelia accumulate intracellular Cl<sup>−</sup> against an electrochemical gradient. In principle, such accumulation could proceed by coupling directly to a source of metabolic energy or indirectly through a symport or antiport mechanism to flows of other diffusible moieties. A considerable body of evidence now suggests that electroneutral transfer of NaCl is an important mechanism for Cl<sup>−</sup> transport in a number of leaky epithelia (Duffey, Turnheim, Frizzell & Schultz, 1978; Kimura & Spring, 1978; Duffey, Thompson, Frizzell & Schultz, 1979; Frizzell, Field & Schultz, 1979; Reuss & Grady, 1979). Whether NaCl cotransport also proceeds in frog skin and toad bladder is less clear. The data currently available suggest that in these tissues, Cl<sup>−</sup> is more appropriately modeled by introducing a Cl<sup>−</sup> pump than a NaCl symport mechanism (Finn, Handler & Orloff, 1967; Davies, Martin & Sharp, 1968; Biber, Walker & Mullen, 1980). The choice of an apparent dissociation constant in Eq. (10) of 2 mM for the hypothetical Cl<sup>−</sup> site complex was guided by the recent data of Biber et al. (1980).

Equation (11) is a statement of electroneutrality in each of the three compartments of the model;  $X^{*x}$  is constrained solely to the intracellular phase. Equation (12) is a statement of osmotic equilibrium across the basolateral plasma membrane. Equation (13) states that over the time frame of interest, capacitative currents are negligible. Equation (14) takes note of the fact that transepithelial current ( $I_T$ ) may be carried through both transcellular ( $I_S^{cell}$ ) and paracellular ( $I_S^{cm}$ ) pathways.

Equations (15)–(19) are not involved in the algorithm of the model. However, it has been highly instructive to compute the partial ionic conductance of the  $i$ th ion at the  $j$ th barrier ( $g_i^j$ ) by taking the derivative with respect to voltage of the constant field expression for the corresponding partial ionic current [Eq. (1)]. The expression is not defined when the voltage  $E^j$  across the  $j$ th barrier is zero. However, the  $\lim_{E^j \rightarrow 0} g_i^j$  can be determined [Eq. (16)]

by successive applications of l'Hospital's rule. Equations (17)–(19) define the apical ( $G_S^a$ ), basolateral ( $G_S^b$ ), transcellular ( $G_S^{cell}$ ), paracellular ( $G_S^{cm}$ ) and total tissue ( $G_T$ ) conductances.

### Programming Approach

The approach taken by Lew et al., (1979) was followed in the present study. Values based on estimates from the literature were introduced for the first set of parameters:  $P_{Na}^{bl}$  (Helman & Miller, 1974),  $P_{Cl}^{bl}$ ,  $P_{Cl}^a$  (Macchia & Helman, 1976),  $P_i^{jcn}$  (Walser, 1970; Mandel & Curran, 1972; Saito, Lief & Essig, 1974; Civan & DiBona, 1978),  $r$  (Glynn & Karlsh, 1975) and the apparent dissociation constants characterizing the specialized transport sites (Garay & Garrahan, 1973);  $P_K^a$  was chosen to be a small fraction of  $P_K^{bl}$ , as suggested by the data of Robinson and Macknight (1976b). These values were held constant during the computations unless otherwise stated.

Another set of initial baseline values was entered for the second set of parameters:  $I_T$ ,  $V^a$  and  $V^{bl}$  (e.g., Nagel, 1976; Frömter & Gebler, 1977; Helman & Fisher, 1977; Nagel et al., 1980) and  $c_K^c$ ,  $c_{Na}^c$ ,  $c_i^m$ ,  $c_i^c$ , and  $v^c$  (Macknight, DiBona, Leaf & Civan, 1971; Macknight, Civan & Leaf, 1975a,b; Rick et al., 1978b; Civan et al., 1980). All of these parameters were subject to change in response to the experimental perturbations introduced during later periods of the computer simulation. The first two sets of values were unless otherwise stated, the same as those chosen by Lew et al. (1979) to calculate the values of a third set of parameters:  $P_{Na}^a$ ,  $P_K^{bl}$ ,  $(\phi_{Na}^{bl})_{max}$ ,  $(\phi_K^{bl})_{max}$ ,  $c_{Cl}^c$  and  $c_x^c$ , using the expressions entered under "Presentation of Equations Used" above. Thus, the first and third sets of parameters correspond to sets of conventional inputs and outputs, respectively. However, the second set of parameters has a dual role. The initial baseline values provide inputs in order to calculate other parameters, but function as outputs in being responsive to changes in the experimental conditions.

A different strategy was followed for Cl<sup>−</sup> when the model included a Cl-pump at the apical membrane. In this case, the baseline value of  $c_{Cl}^c$  was fixed at 35 mM, as suggested by electron microprobe analysis of toad urinary bladder (Civan et al., 1980). The net influx of Cl<sup>−</sup> through the apical Cl-pump was set equal to the net electrodiffusive efflux of Cl<sup>−</sup> from the cell calculated on the basis of Eq. (1), using the presumed values for  $c_{Cl}^c$ ,  $P_{Cl}^a$  and  $P_{Cl}^{bl}$ .  $(\phi_{Cl}^a)_{max}$  could then be calculated from Eq. (10).

Following each change in experimental conditions, all of the variable parameters were recalculated. These included:  $c_i^c$ ,  $v^c$ ,  $V^a$ ,  $V^{bl}$ ,  $I_i^j$  and either  $V^{jcn}$  or  $I_T$ , depending on whether current or voltage was being clamped. The two major steps in the computation were the numerical solutions of the constant field equations relating the total current across the apical membrane ( $I_S^a$ ) to  $V^a$  and relating the total current across the basolateral membrane ( $I_S^b$ ) to  $V^{bl}$ . These computations were performed by application of the Newton-Raphson method and solving the two simultaneous differential equations by a fourth-order Runge-Kutta method. It should be emphasized that the algorithm used was entirely that developed by Lew, Ferreira and Moura (1979), whose paper should be consulted for further details.

Although the programmatic approach is no different than that used previously, we have found it highly instructive additionally to calculate and print out the partial ionic currents and conductances as well as the total conductances across each of the permeability barriers, using the equations presented above. In addition to the 10 parameters followed by Lew et al. (1979), we have monitored 20 other functions. For purposes of clarity, only some of the parameters followed are presented in the "Results".

### Computer Facilities

Three computers (Digital Equipment Corp., Maynard, Mass.) were used in the present work: (i) our own LSI-11/03 with 64 kb

**Table 1.** The transition from short to open circuit<sup>a</sup>

Condition	Time (min)	$c_{\text{Na}}^i$ (mM)	$F(\phi_{\text{Na}}^{bl})$ ( $\mu\text{A cm}^{-2}$ )	$(I_{\text{Na}})_T$	$G_{\Sigma}^a$	$G_{\Sigma}^{\text{cell}}$	$G_T$	$E^a$ (mV)	$E^{jn}$
Short circuit	0.0	20.00	27.50	25.00	281.2	225.8	366.4	80.85	0.00
Open circuit	0.0	20.00	27.50	9.32	234.7	183.2	323.7	24.14	-71.80
	0.2	18.38	26.31	9.34	233.3	182.8	323.3	23.94	-71.82
	0.4	16.91	25.10	9.35	232.0	182.5	323.0	23.73	-71.82
	0.6	15.60	23.90	9.36	230.8	182.2	322.7	23.54	-71.80
	0.8	14.43	22.74	9.36	229.7	181.9	322.5	23.35	-71.76
	1.0	13.40	21.62	9.37	228.7	181.7	322.2	23.17	-71.70
	1.2	12.51	20.57	9.37	227.9	181.5	322.0	23.00	-71.64
	1.4	11.74	19.61	9.37	227.1	181.3	321.9	22.86	-71.58
	1.6	11.08	18.74	9.37	226.5	181.2	321.7	22.72	-71.52
	1.8	10.53	17.96	9.37	225.9	181.1	321.6	22.60	-71.46
	2.0	10.06	17.29	9.37	225.4	181.0	321.5	22.50	-71.41
	2.4	9.35	16.20	9.37	224.7	180.8	321.4	22.34	-71.31
	3.0	8.69	15.13	9.36	224.0	180.7	321.2	22.19	-71.22
	4.0	8.20	14.29	9.36	223.5	180.6	321.1	22.06	-71.14
	5.0	8.03	13.99	9.36	223.3	180.5	321.1	22.02	-71.11
	6.0	7.97	13.89	9.36	223.2	180.5	321.1	22.00	-71.10
	8.0	7.94	13.84	9.36	223.2	180.5	321.1	22.00	-71.10
	10.0	7.94	13.83	9.36	223.2	180.5	321.1	22.00	-71.10
	65.0	7.94	13.83	9.36	223.2	180.5	321.1	21.99	-71.10
	183.0	7.94	13.83	9.36	223.2	180.5	321.1	21.99	-71.10

<sup>a</sup> The parameters have been calculated using the basic model of Lew, Ferreira and Moura (1979), setting  $P_{\text{Cl}}^a = 1.9 \times 10^{-8} \text{ cm sec}^{-1}$  and  $\sigma_{\text{KCl}} = 1.00$ . Under these conditions, cell volume is computed to remain constant throughout the simulation. Of the total rate of net Na<sup>+</sup> entry into the cell, 9.1% proceeds across the basolateral membrane under short-circuited conditions and 21.0% initially in the open circuit, decaying slightly to 20.6% in the steady state.

of memory; (ii) a PDP-11/34 with a floating point processor, kindly made available to us by Dr. Stephen Baylor; and (iii) the PDP-10 of the Computing Facility of the University of Pennsylvania School of Medicine. The fourth-order Runge-Kutta method was implemented with a subroutine available in many scientific subroutine packages.

For those readers who are considering acquiring a computer facility for the purposes of the present study, it will be of interest to note the relative computation times for the three facilities. The same computer simulation required 73 min with the LSI-11/03, 2.4 min with the PDP-11/34, and 5 sec with the PDP-10.

Figures were constructed with the assistance of a graphics plotter (Model HP-7221B, Hewlett-Packard, San Diego, Calif.).

## Results

### Transition from Short-circuited to Open-circuited State

In view of the equivalence reported for net sodium transport and short-circuit current across frog skin (Ussing & Zerahn, 1951) and toad urinary bladder (Leaf, Anderson & Page, 1958), most studies of these epithelial preparations have been conducted under short-circuited conditions. On the other hand, the physiologically relevant state is the open-circuited condition. It is therefore of particular interest to examine the changes in the concentration, potential and conductance profiles associated with the transition between these two transport states.

As reported by Lew et al. (1979), open-circuiting their basic model results in a modest hyperpolarization of the basolateral membrane, a marked depolarization of the apical membrane, and cell swelling (Table 1, Fig. 1). Although the changes in polarization are not unexpected, the appearance of swelling is contrary to certain experimental observations. Voûte and Ussing (1968) have reported cellular swelling of the *stratum granulosum* upon short circuiting frog skin. The swelling was more marked when the preparation was further depolarized, reversing the sign of the spontaneous transepithelial potential. Reversing the open-circuit potential has also been found to induce an amiloride-sensitive swelling of the granular cells of toad bladder (Bobycki, Mills, Macknight & Di Bona, 1981). Hviid Larsen (1978) has pointed out that whether or not swelling will be observed following a perturbation depends in part upon the ratio  $P_{\text{Na}}^a/P_{\text{K}}^{bl}$ . In the present study, it has become quite clear that the change in cell volume is also critically dependent upon the apical chloride permeability ( $P_{\text{Cl}}^a$ ).

Figure 1 presents the time course of cell volume associated with the transition from the short-circuited to the open-circuited condition. The three curves have been generated by introducing three different values of  $P_{\text{Cl}}^a$  into the same basic model of

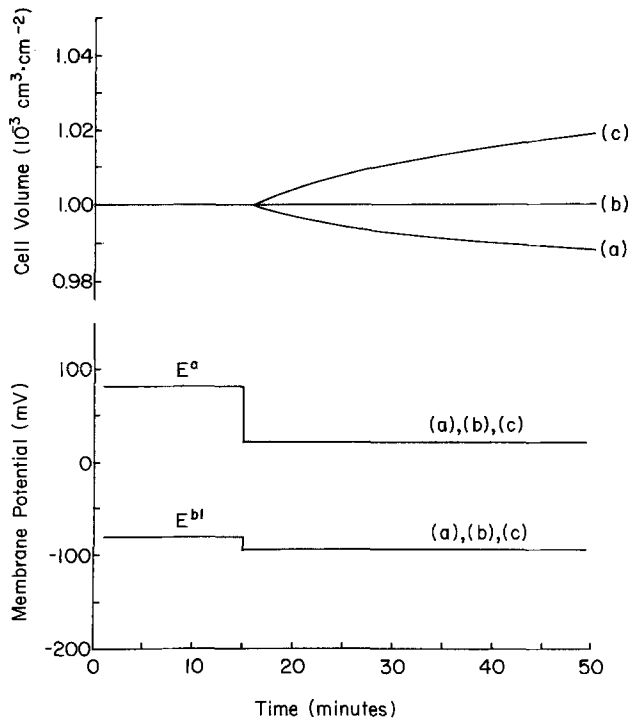


**Fig. 1.** Time dependences of intracellular volume ( $v^i$ ) and apical ( $E^a$ ) and basolateral ( $E^b$ ) membrane potentials during the transition from the short-circuited to the open-circuited state. The curves have been generated by the basic model of Lew, Ferreira and Moura (1979) with  $c_{\text{Na}}^m = 120 \text{ mM}$ , setting  $P_{\text{Cl}}^a$  equal to: (a)  $1.0 \times 10^{-10}$ , (b)  $1.9 \times 10^{-8}$ , and (c)  $5.0 \times 10^{-8} \text{ cm sec}^{-1}$ .

Lew, Ferreira and Moura. As they reported, when  $P_{\text{Cl}}^a = 5 \times 10^{-8} \text{ cm sec}^{-1}$ , swelling is observed. However, no change in volume is noted for  $P_{\text{Cl}}^a = 1.9 \times 10^{-8} \text{ cm sec}^{-1}$ , and shrinkage is actually noted for permeabilities appreciably lower than this value. The model is therefore very useful in helping identify  $P_{\text{Cl}}^a$  as a critical parameter for experimental study in order to adequately characterize cell volume regulation.

The model has also proved helpful in another way as an adjunct to the experimental study of the transition between open circuit and short circuit. At least two sets of experimental data have suggested that the intracellular composition of the epithelial cells of toad bladder is the same in the two voltage states. Chemical analyses of epithelial cell scrapings from toad bladder have been reported to be similar in the two states both under control conditions and in the nominal absence of serosal potassium (Robinson & Macknight, 1976b). Electron microprobe analyses of toad bladder have also suggested that the baseline intracellular concentrations of  $\text{Na}^+$ ,  $\text{K}^+$  and  $\text{Cl}^-$  are similar in the short-circuited (Rick et al., 1978b) and in the open-circuited state (Civan et al., 1980). However, these apparent similarities need not necessarily reflect a true identity of the

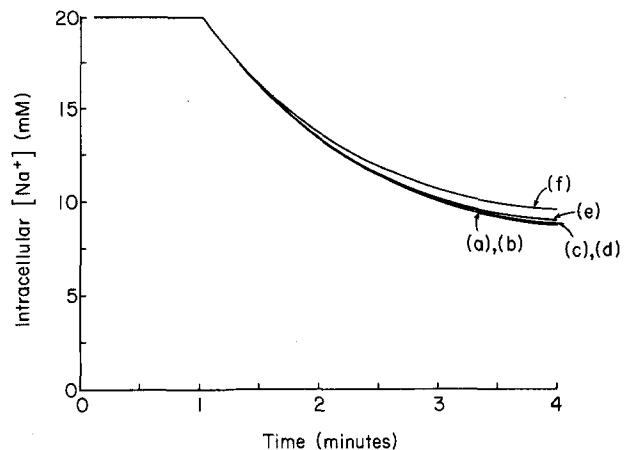


**Fig. 2.** Intracellular  $\text{Na}^+$  concentration ( $c_{\text{Na}}^i$ ) as a function of time, during the transition from short circuit to open circuit, initiated at time = 1 min. Six different graphs have been generated with  $c_{\text{Na}}^m = 120 \text{ mM}$ : (a) Basic model,  $P_{\text{Cl}}^a = 1.0 \times 10^{-10} \text{ cm sec}^{-1}$ ,  $\sigma_{\text{KCl}} = 1.00$ ; (b) Basic model,  $P_{\text{Cl}}^a = 1.9 \times 10^{-8} \text{ cm sec}^{-1}$ ,  $\sigma_{\text{KCl}} = 1.00$ ; (c) Basic model,  $P_{\text{Cl}}^a = 5.0 \times 10^{-8} \text{ cm sec}^{-1}$ ,  $\sigma_{\text{KCl}} = 1.00$ ; (d) Basic model,  $P_{\text{Cl}}^a = 5.0 \times 10^{-8} \text{ cm sec}^{-1}$ ,  $\sigma_{\text{KCl}} = 0.95$ ; (e) Basic model + Cl-pump,  $P_{\text{Cl}}^a = 5 \times 10^{-8} \text{ cm sec}^{-1}$ ,  $\sigma_{\text{KCl}} = 1.00$ ; (f) Modified model incorporating feedback between  $c_{\text{Na}}^i$  and  $P_{\text{Na}}^a$ ,  $P_{\text{Cl}}^a = 5.0 \times 10^{-8} \text{ cm sec}^{-1}$ ,  $\sigma_{\text{KCl}} = 1.00$ .

intracellular composition under these two very different experimental conditions. In preparing the tissues for either chemical or microprobe analysis, the epithelia are necessarily placed in the open-circuited state for substantial fractions of a minute. Given sufficiently rapid rates of exchange, the intracellular composition could relax to that characteristic of open-circuited conditions, irrespective of the tissue composition under voltage-clamped conditions. This would very likely be the case, were the period of time required for preparation very prolonged (e.g.,  $\geq 3 \text{ min}$ , as can be appreciated from the data of Lew et al., 1979). However, given the experimental techniques currently available, the time frame of importance is the interval from 0 to 60 sec following interruption of the voltage clamp.

Figure 2 presents the time course of intracellular sodium concentration during the transition between short circuit and open circuit. Six different experimental conditions are considered. Four curves have been generated with the basic model of Lew et al. (1979), using three different values of  $P_{\text{Cl}}^a$  spanning three orders of magnitude, and in one case, setting  $\sigma_{\text{KCl}} = 0.95$  instead of  $= 1.00$ . A fifth curve reflects operation of the model incorporating a Cl-pump. The sixth curve has been generated with a model discussed below incorporating negative feedback interaction between  $P_{\text{Na}}^a$  and  $c_{\text{Na}}^i$ . The overlap of the graphs suggests that the time course of  $c_{\text{Na}}^i$  is not critically dependent upon the precise choices of parameter and model. After 30 sec and 60 sec,  $c_{\text{Na}}^i$  has

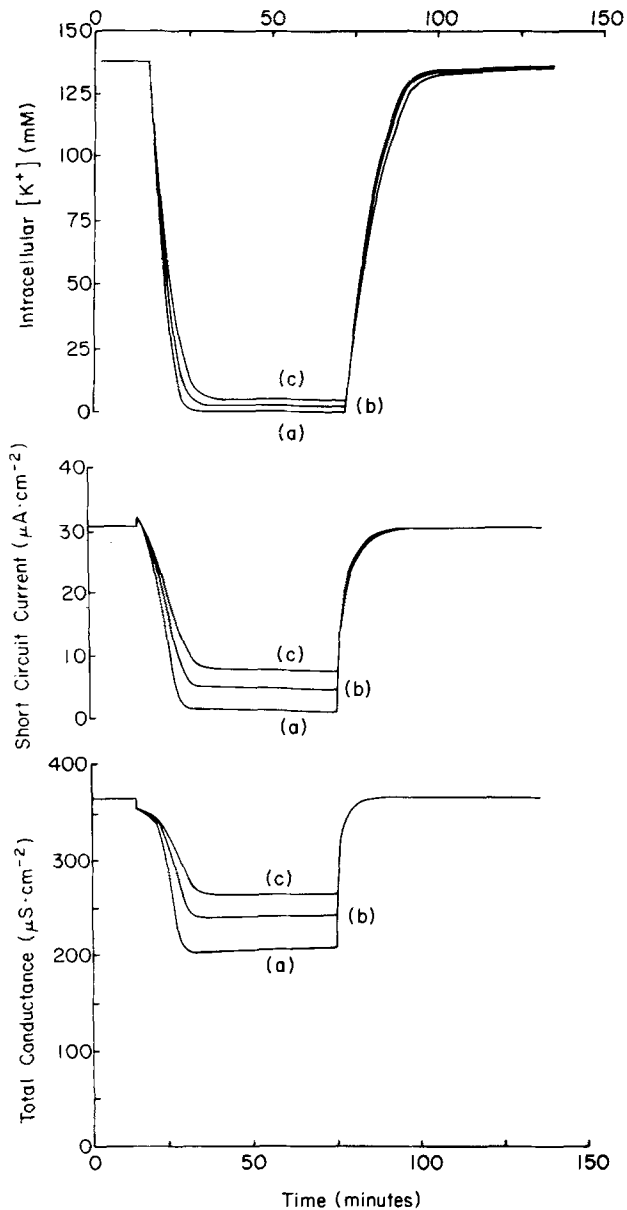


**Fig. 3.** Intracellular  $\text{K}^+$  concentration ( $c_k^i$ ), short-circuit current ( $I_T$ ) and transepithelial conductance ( $G_T$ ) before, during and after transiently reducing the serosal  $\text{K}^+$  concentration ( $c_k^s$ ) during the period in which time = 15–75 min. The graphs have all been generated with the basic model without a  $\text{Cl}^-$ -pump and with  $\sigma_{\text{KCl}} = 1.00$ , in the presence of serosal  $\text{Na}^+$  Ringer's solution, and with  $c_{\text{Na}}^s = 120 \text{ mM}$ , but lowering  $c_k^s$  to the following different values during the experimental period: (a)  $10 \mu\text{M}$  (b)  $0.2 \text{ mM}$ , and (c)  $0.3 \text{ mM}$ . As noted in the text, the value of  $c_k^s$  at the basolateral membrane is likely to lie within the range  $10 \mu\text{M}$ – $0.3 \text{ mM}$  even when toad bladder is bathed with Ringer's solution nominally free of potassium

fallen by 18–19% and by 32–33% respectively, whether the cell has undergone shrinkage or swelling, and whether or not a  $\text{Cl}^-$ -pump is operative.

As may be appreciated from Table 1, the steady-state values of the functional parameters are signifi-

cantly different in the two conditions even with symmetrical bathing media. For example, from a consideration of the basic model, the conductances of the apical and basolateral membranes are expected to be some 20% lower in the open-circuited state. Of particular interest is the observation that recycling of  $\text{Na}^+$  across the basolateral membrane is appreciably more significant under open-circuited conditions. This point will be considered in greater detail later in the "Results" and in the "Discussion".

#### *Reduction of Serosal $\text{K}^+$ Concentration*

A second experimental condition with which this laboratory has been concerned over the past several years has been the lowering of  $c_k^s$ . After briefly stimulating short-circuit current (Essig, 1965; Finn et al., 1967; Robinson & Macknight, 1976a, b), this maneuver reduces the short-circuit current (Essig & Leaf, 1963), intracellular  $\text{K}^+$  concentration (Essig & Leaf, 1963; Robinson & Macknight, 1976b) and transepithelial conductance (DeLong & Civan, 1978) of toad bladder. These effects are qualitatively simulated by the basic model of Lew et al. (1979) (Fig. 3). In addition, reduction of serosal  $\text{K}^+$  concentration is known to hyperpolarize the apical and basolateral membranes of frog skin under short-circuited conditions (Nagel et al., 1980). If the degree and duration of the hyperpolarization are substantial, cell volume undergoes a modest early reduction, consistent with published chemical (Robinson & Macknight, 1976b) and electron microprobe (Civan et al., 1980) measurements of toad bladder. If, however, the hyperpolarization is small and brief, the early fall in cell volume is too small to be detected. Eventually, with loss of approximately a third of the intracellular  $\text{K}^+$ , the membranes become depolarized,  $\text{Cl}^-$  accumulation is initiated, and cell volume progressively increases. The changes in computed cell volume are small, basically because the loss of cellular  $\text{K}^+$  is largely balanced by the gain in  $\text{Na}^+$ , consistent with recent microprobe measurements (Civan et al., 1980).

The basic model also simulates the protective effects of serosal choline in minimizing the adverse sequelae of a reduction in  $c_k^s$ . As first reported by Essig and Leaf (1963) and confirmed by Robinson and Macknight (1976b), the fractional reductions in short-circuit current and  $c_k^i$  induced by lowering  $c_k^s$  are appreciably less marked when choline Ringer's rather than sodium Ringer's solution bathes the serosal surface of toad bladder. This phenomenon was initially considered to reflect a secondary inhibition of  $\text{Na}^+$  entry triggered at the apical membrane by alterations in the composition of the intracellular

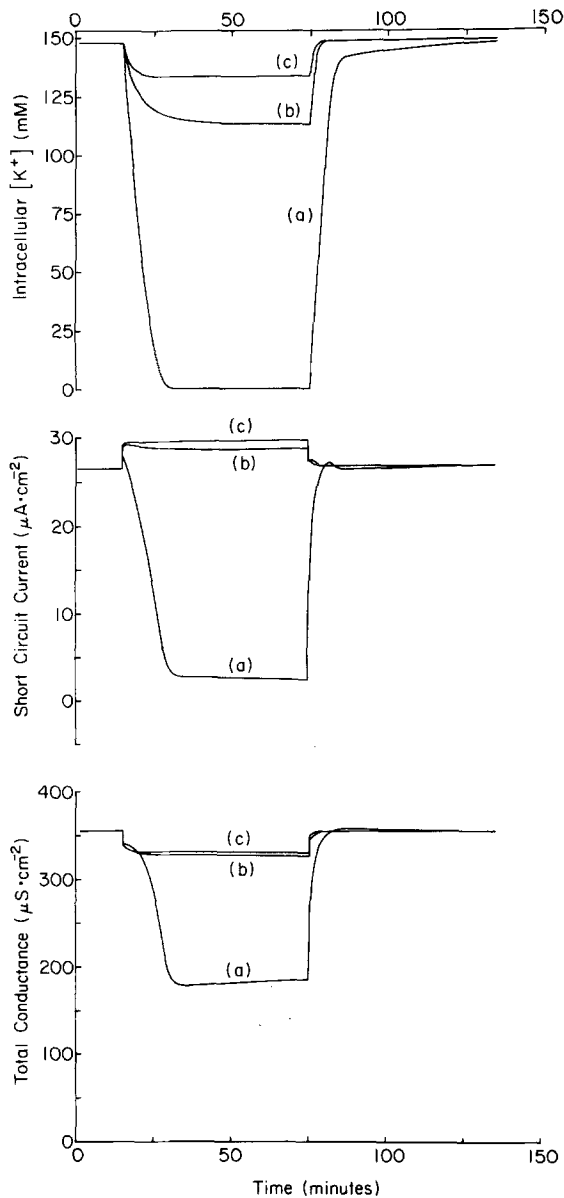


**Fig. 4.** Time courses of  $c_K^i$ ,  $I_T$  and  $G_T$  during the course of reducing and then restoring the serosal  $\text{K}^+$  and  $\text{Na}^+$  concentrations simultaneously. The experimental conditions are identical with those of Fig. 3, except that choline has replaced serosal  $\text{Na}^+$ .

fluids. This hypothesis is very likely correct, but for different reasons considered below. As discussed elsewhere (Civan et al., 1980), the protective effect of choline probably reflects the variable affinity of the outer sites of the  $\text{Na}/\text{K}$ -exchange pump at the basolateral membrane [Eq. (8)]. This concept is presented in quantitative form in Fig. 4.

Although the basic model qualitatively simulates many of the effects elicited by reducing the serosal potassium concentration, it is strikingly unsuccessful in reproducing several other well-documented phenomena. When the serosal surface of toad bladder is

bathed with a sodium Ringer's solution nominally free of  $\text{K}^+$  for 60–90 min, the epithelial cells actually lose only some 20–30% of their total intracellular  $\text{K}^+$  contents (Robinson & Macknight, 1976b; Civan et al., 1980), in contrast to the rapid marked fall in  $c_K^i$  illustrated in Fig. 3. Second, the predicted reduction in transepithelial conductance (Fig. 3) is appreciably less than that observed in toad bladders mounted with minimal edge damage (DeLong & Civan, 1978, 1979). Third, the lag time phenomenon observed by DeLong and Civan (1978, 1979) is entirely absent from the computer simulations of Fig. 3. Specifically, upon restoring serosal potassium to previously potassium-depleted toad bladders, the epithelial cells begin to reaccumulate potassium 20–40 min before any increase in short-circuit current can be measured; by the time that the short-circuit current does begin to climb, the intracellular potassium activity has risen to approximately 90% of its baseline value.

These three defects of the simulation cannot be repaired simply by altering the values of the model parameters in a variety of ways, or even by modifying the model itself by incorporating a chloride pump (Fig. 5). On the other hand, it is possible to provide qualitatively satisfactory simulations by taking account of the negative feedback relationship between  $P_{\text{Na}}^a$  and  $c_{\text{Na}}^i$  suggested by a number of published reports (Erlj & Smith, 1973; Leblanc & Morel, 1975; Morel & Leblanc, 1975; Lewis et al., 1976; Cuthbert & Shum, 1977; Turnheim et al., 1978; Weinstein et al., 1980). This relationship has been introduced into the program by the empirical expressions of Eqs. (3) and (4). For brevity and convenience, we shall refer to the basic model of Lew et al. (1979) incorporating the  $P_{\text{Na}}^a - c_{\text{Na}}^i$  relationship as "the modified program".

Figure 6 presents  $c_K^i$  as a function of time during the course of reducing and restoring the serosal potassium concentration. Each of the curves has been constructed with the modified program, constraining the factor  $f$  [Eq. (4)] not to fall below three different minimal values ( $f_{\min}$ ). The three graphs of Fig. 6 are qualitatively similar in markedly slowing the rates of elution of intracellular potassium. Insofar as the experimental data are more fully simulated when  $f_{\min} = 0.01$ , this value has been used in most of the computer simulations conducted with the modified program.

The crucial importance of the precise value of  $c_K^i$  in the experiment under consideration is illustrated in Fig. 7, a point considered in qualitative terms previously (Civan, *in press*). Although the serosal potassium concentration is commonly lowered experimentally by bathing the serosal surface of toad



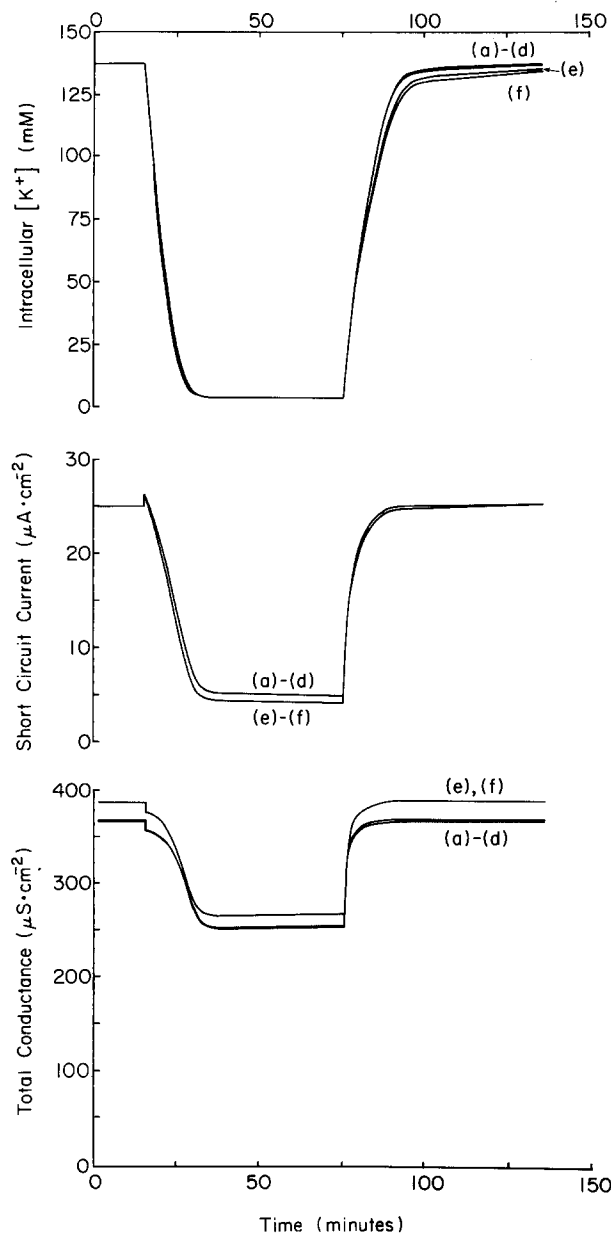


**Fig. 5.** Effects of changes in the basic computer model on the time courses of  $c_K^i$ ,  $I_T$  and  $G_T$  following reduction of  $c_K^s$  to 0.25 mM. The curves have been generated with the basic model in the absence of [(a)-(d)], or incorporating [(e)-(f)], a Cl-pump. (a)  $P_{\text{Cl}}^a = 5 \times 10^{-8} \text{ cm sec}^{-1}$ ;  $\sigma_{\text{KCl}} = 1.00$ ; (b)  $P_{\text{Cl}}^a = 1.9 \times 10^{-8} \text{ cm sec}^{-1}$ ;  $\sigma_{\text{KCl}} = 1.00$ ; (c)  $P_{\text{Cl}}^a = 1.0 \times 10^{-10} \text{ cm sec}^{-1}$ ;  $\sigma_{\text{KCl}} = 1.00$ ; (d)  $P_{\text{Cl}}^a = 5.0 \times 10^{-8} \text{ cm sec}^{-1}$ ;  $\sigma_{\text{KCl}} = 0.95$ ; (e)  $P_{\text{Cl}}^a = 5 \times 10^{-8} \text{ cm sec}^{-1}$ ;  $\sigma_{\text{KCl}} = 0.95$ ; (f)  $P_{\text{Cl}}^a = 5.0 \times 10^{-8} \text{ cm sec}^{-1}$ ;  $\sigma_{\text{KCl}} = 1.00$

bladder or frog skin with solutions nominally free of potassium, measured values of  $c_K^s$  have been reported to be as high as 0.2 mM (Robinson & MacKnight, 1976b). Thus, the range of values considered for  $c_K^s$ , from 10  $\mu\text{M}$  to 0.3 mM, is experimentally relevant. Of particular interest is the result that, following an initial drop of 20.7%,  $c_K^i$  began to climb

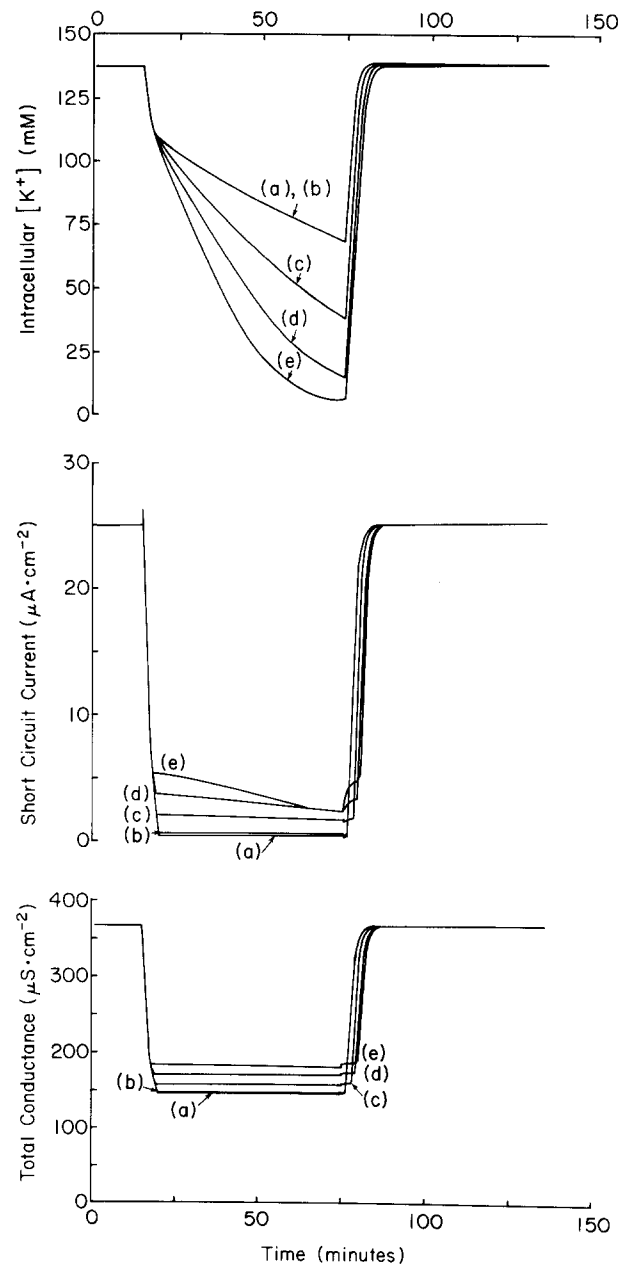


**Fig. 6.** Time courses of  $c_K^i$ ,  $I_T$  and  $G_T$  during the course of reducing  $c_K^s$  to 0.2 mM predicted by the modified program. The curves differ only in the minimum value which the factor  $f$  can assume: (a) 0.005, (b) 0.01, (c) 0.05, (d) 0.10 and (e) 0.15

slightly towards its baseline value, despite the continued presence of only 0.3 mM potassium in the serosal bath. Thus, in this case, even in the absence of cellular heterogeneity, intracellular compartmentalization or subcellular binding,  $c_K^i$  is expected to fall by no more than 20% after an hour's incubation.

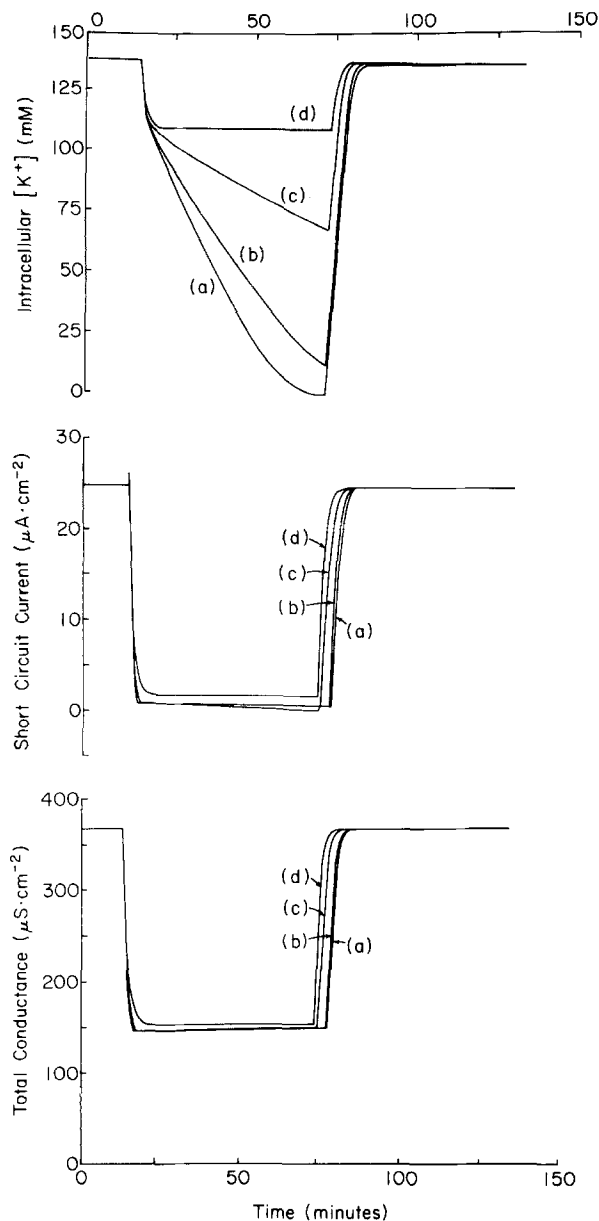


Fig. 7. Time courses of  $c_K^s$ ,  $I_T$  and  $G_T$  associated with reducing  $c_K^s$  to: (a) 10  $\mu\text{M}$ , (b) 0.1 mM, (c) 0.2 mM, and (d) 0.3 mM, predicted by the modified program with  $f_{\min}=0.01$

The values computed for tissue conductance with the modified program are also much more in line with the experimental results of DeLong and Civan (1978, 1979) who observed severalfold falls in this parameter following reduction of serosal potassium concentration. For example, when  $c_K^s=0.2$  mM, the tissue conductance falls from the baseline value by a factor of 2.5 using the modified program (Fig. 7), in comparison to a factor of only 1.5 on the basis of the basic program (Fig. 3).

Perhaps the most striking result generated by the modified program is that illustrated by Fig. 8. This

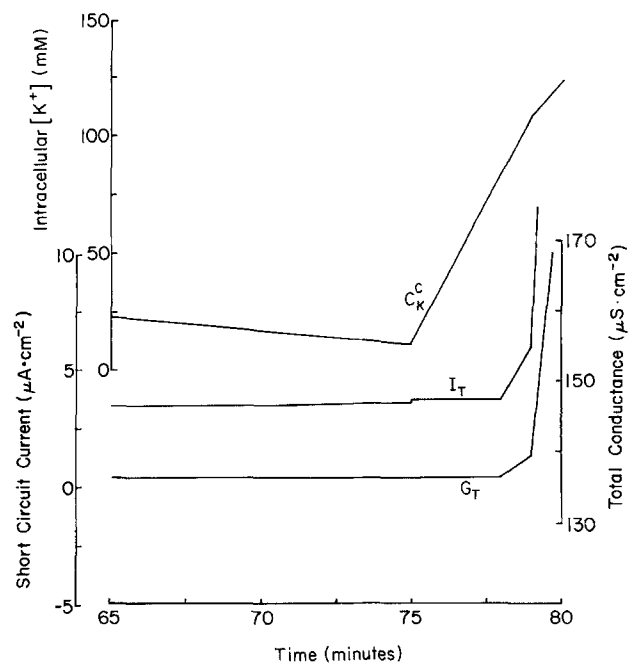
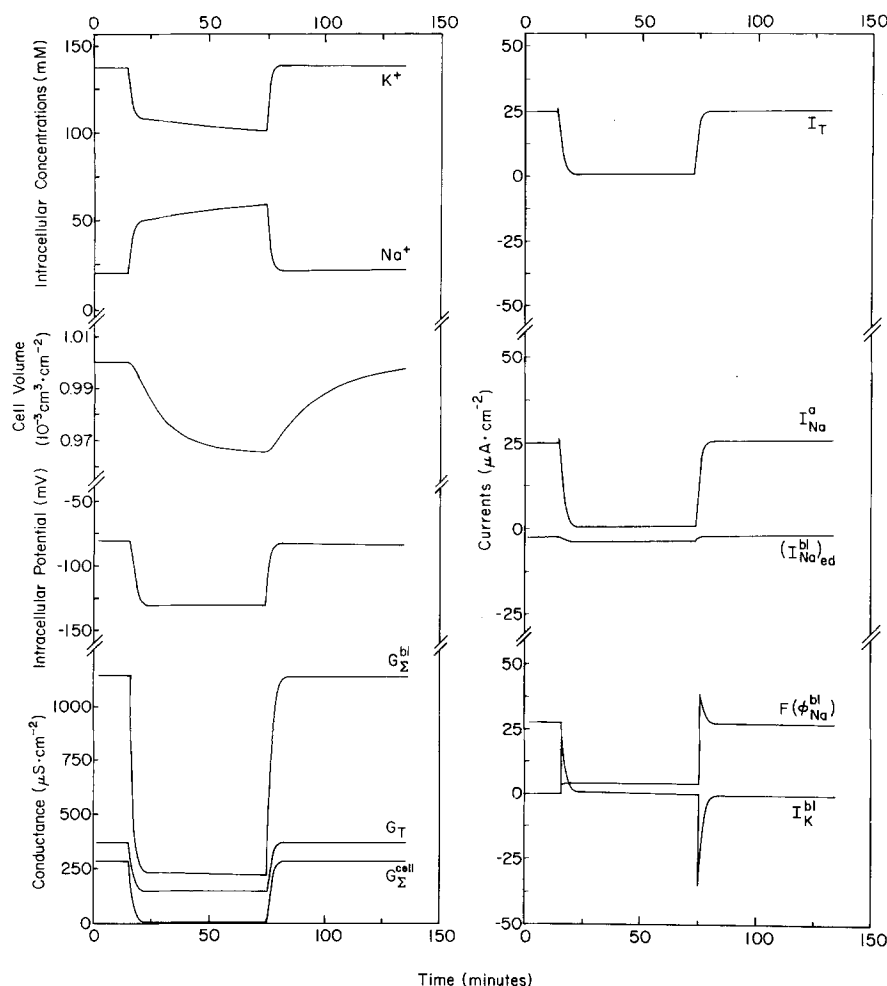


Fig. 8. Lag time between onset of recovery for  $c_K^s$  and that for  $I_T$  and  $G_T$  predicted by the modified program following restoration of  $c_K^s$  from 0.1 to 2.5 mM

Figure presents the intracellular potassium concentration, short-circuit current and tissue conductance of Fig. 7, before and after elevating  $c_K^s$  from 0.2 to 2.5 mM, using an expanded time scale. As experimentally observed, restoration of potassium to the serosal bath leads to a reaccumulation of cellular potassium appreciably before the short-circuit current and tissue conductance begin to increase. Despite the qualitative agreement with experiment, the magnitude of the simulated lag time is some five times smaller than that actually observed. This is not particularly surprising, since the factor  $f$  has been expressed as a direct function of intracellular sodium concentration. It is more likely that the negative feedback between  $P_{\text{Na}}^a$  and  $c_{\text{Na}}^s$  is indirect, mediated possibly by changes in the intracellular calcium activity elicited by changes in  $c_{\text{Na}}^s$  (Grinstein & Elij, 1978; Taylor & Windhager, 1979). If correct, this mechanism would necessarily introduce a further time delay between the onset of reaccumulation of cell potassium (and extrusion of cell sodium) and the onset of the increase in short-circuit current. In the absence of further, more concrete information concerning the response time of the putative coupling, further alterations in the modified model seem inappropriate at present.

Figure 9 presents a more complete picture of the effects of reducing  $c_K^s$  by providing the time courses of a larger number of variables [ $c_K^s$ ,  $c_{\text{Na}}^s$ ,  $v^c$ ,  $I_T$ ,  $I_{\text{Na}}^a$ , the electrodiffusive component ( $I_{\text{Na}}^{bl}$ ) of  $I_{\text{Na}}^a$ ,  $F(\phi_{\text{Na}}^{bl})$ ,



**Fig. 9.** Time courses of intracellular concentrations, ionic currents and conductances during course of transiently reducing  $c_K^s$  to 0.25 mM. The graphs have been generated with the modified program, setting  $P_{Cl}^a = 5.0 \times 10^{-8} \text{ cm sec}^{-1}$  and  $\sigma_{KCl} = 1.00$ , in the absence of a Cl-pump

$I_K^{bl}$ ,  $G_\Sigma^a$ ,  $G_\Sigma^{bl}$  and  $G_T$ ] describing a single experimental situation. The graphs have been generated with the modified program in the absence of a chloride pump, using the assumed initial values of Lew et al. (1979), and setting  $\sigma_{KCl} = 1$ . Upon reducing the serosal potassium concentration by an order of magnitude, from 2.5 to 0.25 mM,  $c_K^s$  falls sharply at first. However, the loss of potassium is largely counterbalanced by the gain in intracellular sodium. Because of the interaction between  $P_{Na}^a$  and  $c_{Na}^i$  in the modified program, the rise in intracellular sodium reduces the rate of further apical  $\text{Na}^+$  entry, sharply decreasing the rate of further loss of intracellular potassium. At the conclusion of the hour's incubation in the presence of a reduced serosal  $\text{K}^+$  concentration, the cells have lost only 29.5% of their total  $\text{K}^+$  contents. Because of the slight fall in cell volume,  $c_K^i$  was reduced even less, by 27.0%.

As previously described (Essig, 1965; Ussing, 1965; Finn et al., 1967; Robinson & Macknight, 1976a), reduction of  $c_K^s$  was associated with a transient increase in the short-circuit current (Fig. 9),

although the magnitude of the simulated effect is less than that actually observed. In the computer simulation, the phenomenon reflects the very rapid initial loss of  $\text{K}^+$  from the cell into the serosal medium despite the abrupt fall in active  $\text{Na}^+$  transport by the basolateral pump. The charge transfer across the basolateral membrane is balanced by an equivalent current carried by  $\text{Na}^+$  from the mucosal medium into the cell, resulting in a similar transient stimulation of  $I_{Na}^a$  following reduction in  $c_K^s$  (Fig. 9). Both  $I_{Na}^a$  and  $I_K^{bl}$  decay relatively rapidly with time. It will be appreciated that the rate of sodium extrusion recovers slightly, following the sharp initial decline; this effect arises from the increase in  $c_{Na}^i$  and the reduction in  $c_K^i$ , enhancing the probability of  $\text{Na}^+$  occupancy at the inner sites of the Na/K-exchange pump.

The comparison of  $I_{Na}^a$  with the electrodiffusive component ( $I_{Na}^{bl})_{ed}$  of  $I_{Na}^{bl}$  in Fig. 9 is of considerable interest. Within 7 min after reducing  $c_K^s$ , the rate of apical sodium entry has fallen to <2% of its baseline value, while the rate of basolateral entry ac-

**Table 2.** Transitions between the short- and open-circuited states in the presence of high (120 mM) and low (1.8 mM) mucosal Na<sup>+</sup> concentrations<sup>a</sup>

$c_{Na}^m$ (mM)	Time (min)	$c_{Na}^e$ (mM)	$c_K^e$ (mM)	$v^e$ (10 <sup>-3</sup> cm <sup>3</sup> cm <sup>-2</sup> )	$E^{bl}$ (mV)	$E^{jen}$ (mV)	$(I_{Na}^{bl})$	$F(\phi_{Na}^{bl})$ (μA cm <sup>-2</sup> )	$(I_{Na})_T$	$I_T$	$G_s^a$ (μS cm <sup>-2</sup> )	$G_s^{cell}$ (μS cm <sup>-2</sup> )	$G_T$
120.00	0	20.00	137.50	1.0000	80.85	0.00	25.00	27.50	25.00	24.90	283.2	227.10	367.6
120.00	0	20.00	137.50	1.0000	15.46	-83.24	24.50	27.50	23.22	0.00	230.7	178.4	272.8
	1	12.81	144.65	1.0014	7.80	-88.84	18.00	20.94	16.63	0.00	258.1	198.2	292.5
	2	9.50	147.90	1.0030	4.39	-90.87	13.53	16.44	12.13	0.00	267.0	205.6	300.0
	5	7.74	149.47	1.0083	2.58	-91.75	10.62	13.50	9.21	0.00	270.6	209.1	303.4
	10	7.67	149.29	1.0159	2.46	-91.73	10.51	13.39	9.10	0.00	270.6	209.2	303.6
	20	7.64	148.93	1.0272	2.37	-91.67	10.51	13.38	9.10	0.00	270.6	209.3	303.7
	40	7.62	148.54	1.0401	2.27	-91.60	10.50	13.37	9.09	0.00	270.6	209.4	303.8
	50	7.61	148.43	1.0436	2.25	-91.58	10.49	13.36	9.09	0.00	270.5	209.5	303.8
	60	7.60	148.35	1.0461	2.23	-91.57	10.49	13.36	9.08	0.00	270.5	209.5	303.8
1.8	60	7.60	148.35	1.0461	51.13	-52.38	10.22	13.36	9.30	0.00	63.0	58.2	88.2
	61	4.38	151.69	1.0427	44.58	-56.53	3.67	6.74	2.70	0.00	58.5	54.5	83.5
	62	3.52	152.64	1.0396	42.54	-57.93	1.78	4.84	0.79	0.00	56.5	52.9	81.5
	65	3.24	153.21	1.0312	41.95	-58.40	1.14	4.20	0.15	0.00	55.6	52.1	80.6
	70	3.24	153.59	1.0194	42.21	-58.33	1.14	4.20	0.14	0.00	55.4	51.9	80.4
	80	3.26	154.15	1.0026	42.60	-58.20	1.15	4.21	0.15	0.00	55.1	51.6	80.1
	100	3.28	154.73	0.9855	43.01	-58.07	1.16	4.23	0.17	0.00	54.7	51.3	79.8
	110	3.29	154.87	0.9816	43.11	-58.04	1.16	4.23	0.17	0.00	54.7	51.2	79.8
	120	3.29	154.96	0.9791	43.17	-58.02	1.16	4.24	0.17	0.00	54.6	51.2	79.7
1.8	120	3.29	154.96	0.9791	98.21	0.00	1.24	4.24	0.86	4.70	39.3	37.6	86.1
	121	3.94	154.31	0.9789	98.71	0.00	2.66	5.66	2.27	4.65	39.4	37.7	86.2
	122	4.10	154.16	0.9786	98.84	0.00	3.00	6.01	2.62	4.64	39.5	37.7	86.2
	125	4.15	154.13	0.9780	98.89	0.00	3.11	6.12	2.72	4.63	39.5	37.7	86.2
	130	4.15	154.16	0.9772	98.89	0.00	3.11	6.12	2.73	4.63	39.4	37.7	86.2
	140	4.16	154.20	0.9761	98.92	0.00	3.11	6.12	2.73	4.63	39.4	37.7	86.1
	160	4.16	154.24	0.9750	98.94	0.00	3.11	6.12	2.73	4.63	39.4	37.6	86.1
	170	4.16	154.25	0.9748	98.95	0.00	3.11	6.12	2.73	4.63	39.4	37.6	86.1
	180	4.16	154.25	0.9747	98.95	0.00	3.11	6.12	2.73	4.63	39.4	37.6	86.1

<sup>a</sup> Values have been predicted on the basis of the modified model in the absence of a Cl-pump, and with  $\sigma_{KCl}=1.00$ . When  $c_{Na}^m=1.8$  mM,  $c_K^m$  has been set equal to 1.5 mM, and  $c_{Cl}^m=3.3$  mM. The junctional permeabilities for Na<sup>+</sup>, Cl<sup>-</sup> and K<sup>+</sup> have been fixed at  $3.4 \times 10^{-7}$ ,  $1.7 \times 10^{-7}$  and  $4.7 \times 10^{-8}$  cm sec<sup>-1</sup>, respectively.

tually increases because of hyperpolarization of the basolateral membrane by some 50 mV. Because of these altered flux rates, the rate of Na<sup>+</sup> entry across the basolateral membrane becomes an order of magnitude greater than that across the mucosal membrane.

The conductance changes elicited by reducing  $c_K^s$  to 0.25 mM are also presented in Fig. 9. The hyperpolarization of the basolateral membrane and the fall in  $c_K^e$  lead to a marked reduction in both the partial ionic conductance of K<sup>+</sup> and the total membrane conductance of the serosal membrane. However, because of the operation of the negative feedback mechanism of the modified program, the absolute value of the total conductance of the apical membrane is reduced even more strikingly to only 5 μS cm<sup>-2</sup>. Under these circumstances, the total conductance for the entire tissue consists almost entirely of the conductance provided by the paracellular transepithelial pathway (Fig. 9).

Upon restoring potassium to the serosal medium in Fig. 9, all of the changes noted above are re-

versed, the preparation returning to its baseline state. Insofar as  $c_K^s$  was returned to 2.5 mM before the intracellular sodium concentration had assumed very high values, the lag time between restoration of  $c_K^e$  and  $I_T$  is very small.

#### Reduction of Mucosal Na<sup>+</sup> Concentration

A third major experimental concern of this laboratory has been the possible role of the intercellular limiting or tight junctions in regulating net Na<sup>+</sup> transport across tight as well as leaky epithelia (DiBona & Civan, 1973; Civan & DiBona, 1974, 1978). Civan and DiBona (1978) have reported that lowering the mucosal osmolality ( $\pi^m$ ) from 218–226 to 26–27 mOsm · (kg water)<sup>-1</sup> reduces the junctional Na<sup>+</sup> permeability of toad bladder by a factor of 1.49; this phenomenon was considered to have a physiologic role in conserving urinary loss of NaCl. Reuss and Finn (1975) came to a similar conclusion, but, on the basis of their electrophysiologic data, ascribed the junctional effect to a

**Table 3.** Net Na<sup>+</sup> transport across basolateral membrane ( $I_{Na}^{bl}$ ) and net Na<sup>+</sup> reabsorption across entire preparation [ $(I_{Na})_T$ ] under open-circuited conditions

Model	$\sigma_{KCl}$	Junctional permeabilities	Mucosal Na <sup>+</sup> concentration (mm)									
			120.0		11.5		1.8		1.0		0.1	
			$I_{Na}^{bl}$	$(I_{Na})_T$	$I_{Na}^{bl}$	$(I_{Na})_T$	$I_{Na}^{bl}$	$(I_{Na})_T$	$I_{Na}^{bl}$	$(I_{Na})_T$	$I_{Na}^{bl}$	$(I_{Na})_T$
Basic	1.00	high	11.1	9.5	3.4	1.6	1.0	-0.3	0.5	-0.7	-0.1	-1.1
		low	9.2	8.0	2.9	1.6	0.9	0.0	0.5	-0.3	-0.1	-0.7
	0.95	high	11.1	9.5	3.4	1.6	1.0	-0.3	0.5	-0.7	-0.1	-1.1
		low	9.2	8.0	2.9	1.6	0.9	0.0	0.5	-0.3	-0.1	-0.7
Modified	1.00	high	12.6	10.8	4.0	2.0	1.3	-0.1	0.8	-0.5	-0.1	-1.1
		low	10.5	9.1	3.4	2.0	1.2	0.2	0.7	-0.2	-0.1	-0.8
	0.95	high	12.6	10.8	4.0	2.0	1.3	-0.1	0.8	-0.5	-0.1	-1.1
		low	10.5	9.1	3.4	2.0	1.2	0.2	0.7	-0.2	-0.1	-0.8
Basic + Cl-Pump	1.00	high	12.5	10.9	4.4	2.8	1.4	0.3	0.7	-0.4	-0.1	-1.1
		low	10.6	9.5	4.1	2.9	1.4	0.6	0.7	0.0	-0.1	-0.7
	0.95	high	12.5	10.9	4.4	2.8	1.4	0.3	0.7	-0.4	-0.1	-1.1
		low	10.7	9.5	4.0	2.9	1.4	0.6	0.7	0.0	-0.05	-0.7
Modified + Cl-Pump	1.00	high	14.1	12.3	5.2	3.4	1.8	0.6	1.0	-0.2	-0.1	-1.7
		low	12.0	10.6	4.6	3.4	1.8	1.0	1.0	0.2	-0.1	-0.7
	0.95	high	14.1	12.3	5.2	3.4	1.8	0.6	1.0	-0.2	-0.1	-1.1
		low	12.0	10.6	4.6	3.4	1.8	1.0	1.0	0.2	-0.1	-0.7

dependence on  $c_{Na}^m$ . Although the effects of mucosal nonelectrolytes on transepithelial electrical resistance (Civan & DiBone, 1978) now suggest that the junctions respond to gradients in osmolality, rather than in Na<sup>+</sup> concentration,  $c_{Na}^m$  and  $\pi^m$  commonly vary in parallel *in vivo*.

Conclusions concerning the possible physiologic regulatory role of the apical junctions have been reached on the basis of linear equivalent circuit models. This problem has now been reexamined using the nonlinear models considered in the present study.

In this part of the work, each simulation consisted of five sequential experimental periods of 60 min each: (1) The experiment was initiated by short-circuiting the tissue in the presence of identical mucosal and serosal media with  $c_{Na}^m = 120$  mm. (2) Conditions were unchanged, other than to reduce  $P_{Cl}^a$  from  $5 \times 10^{-8}$  cm sec<sup>-1</sup> to  $5 \times 10^{-10}$  cm sec<sup>-1</sup> in some of the simulations. (3) The tissue was open-circuited. (4)  $c_{Na}^m$  was reduced to one of four possible lower concentrations (11.5, 1.8, 1.0 or 0.1 mm) (Table 4) in the open-circuited state. The value of 11.5 mm was chosen to simulate the conditions of Civan and DiBona (1978). The concentration of 1.8 mm is the lowest value reported for toad urine *in vivo* (Sawyer, 1956; Leaf et al., 1958). The values of 1.0 and 0.1 have been used to facilitate comparison with the computations of Lew et al. (1979). In each case,  $c_{Cl}^m$  was lowered by the same amount. (5) The preparation was short-circuited in the presence of

the same low mucosal Na<sup>+</sup> concentration as in period 4. For each simulation, the junctional permeabilities were taken to have the values either entered in the Materials and Methods ("high" junctional permeabilities) or values 1.49 times lower ("low" junctional permeabilities), conforming to the results of Civan and DiBona (1978).

Table 2 presents some of the information obtained with one such experimental simulation. For simplicity, only 13 of the monitored parameters are tabulated at the 19 time points specified. As can be appreciated from the Table, the parameters were satisfactorily close to the final steady state at the end of each period of 60 min. These values computed at the conclusion of each experimental period were then used to construct Tables 3 and 4. The effects of reducing  $\pi^m$  and  $c_{Na}^m$  were studied with both the basic model of Lew et al. (1979) and the current modified model incorporating negative feedback between  $P_{Na}^a$  and  $c_{Na}^m$ , in each case with and without a Cl-pump and with  $\sigma_{KCl}$  set to 1.00 and 0.95 in alternate simulations. In most of the experiments,  $P_{Cl}^a$  was also set alternately equal to  $5 \times 10^{-8}$  cm sec<sup>-1</sup> and  $5 \times 10^{-10}$  cm sec<sup>-1</sup>; insofar as no significant difference was noted, only the results obtained with the former value [the baseline value of Lew et al. (1979)] are entered in Tables 3 and 4.

The most striking aspect of these simulations is that all of the models generate stable results, even when net transepithelial Na<sup>+</sup> movement ( $(I_{Na})_T$ ) proceeds from serosa to mucosa. Second, it is clear that

**Table 4.** Intracellular Na<sup>+</sup> concentration ( $c_{\text{Na}}^i$ ), net Na<sup>+</sup> reabsorption [ $(I_{\text{Na}})_T$ ] and total current ( $I_T$ ) under short- and open-circuited conditions with (+) and without (−) a Cl-pump<sup>a</sup>

Condition	$c_{\text{Na}}^m$	$c_{\text{Cl}}^m$	$c_{\text{K}}^m$	$c_{\text{Na}}^i$	(mm)	$(I_{\text{Na}})_T$	$(\mu\text{A cm}^{-2})$	$I_T$	$(\mu\text{A cm}^{-2})$
		(mm)		(−)	(+)	(−)	(+)	(−)	(+)
Short-circuited	120.0	122.5	2.5	20.0	20.0	25.0	26.7	24.9	24.9
	11.5	14.0	2.5	9.1	9.2	12.5	13.4	14.3	13.6
	1.8	3.3	1.5	4.2	4.3	2.7	2.9	4.6	1.8
	1.0	1.01	0.01	3.6	3.8	0.9	1.1	3.3	2.8
	0.1	0.11	0.01	2.8	3.0	−0.6	−0.5	1.6	1.5
Open-circuited:	120.0	122.5	2.5	8.8	9.1	10.8	12.4	0	0
	11.5	14.0	2.5	4.3	4.8	2.0	3.4	0	0
	1.8	3.3	1.5	3.3	3.6	0.2	1.0	0	0
	1.0	1.01	0.01	3.1	3.3	−0.2	0.2	0	0
	0.1	0.11	0.01	2.7	2.9	−0.8	−0.7	0	0

<sup>a</sup> Computations have been generated with the modified program, setting  $\sigma_{\text{KCl}} = 1.00$  and  $P_{\text{Cl}}^a = 5 \times 10^{-8}$  cm sec<sup>−1</sup>. With  $c_{\text{Na}}^m = 120$  mm, the junctional permeabilities are 1.49 times larger than those associated with the hypoosmotic media.

altering the junctional permeabilities by only 49% exerts a modest but highly significant effect on net Na<sup>+</sup> reabsorption. If the junctional permeabilities were unresponsive to  $c_{\text{Na}}^m$  (first line of Table 3), the basic model predicts a net loss of Na<sup>+</sup> by toad bladder into the urine, even when  $c_{\text{Na}}^m$  remains in the physiologic range (1.8 mm). On the other hand, when account is taken of the documented responsiveness of the junctions to  $\pi^m$  (Civan & DiBona, 1978), the basic model predicts net Na<sup>+</sup> balance at the same value of  $c_{\text{Na}}^m$  (second line of Table 3). An even more favorable result is generated by means of the modified program (lines 5–8 of Table 3); positive net Na<sup>+</sup> balance is sustained down to values of  $c_{\text{Na}}^m < 1.8$  mm, albeit  $> 1.0$  mm, when the junctional permeabilities are set at the lower values.

As expected, the incorporation of a Cl-pump permits the epithelium to reabsorb Na<sup>+</sup> more effectively. The simulation generated by the basic model predicts zero net Na<sup>+</sup> balance for  $c_{\text{Na}}^m = 1.0$  mm (lines 10 and 12 of Table 3), while the modified model results in persistent net Na<sup>+</sup> reabsorption at this dilution, so long as the junctional permeabilities are responsive to  $\pi^m$  (lines 14 and 16 of Table 3). In the latter case, the maximum chemical gradient against which net Na<sup>+</sup> reabsorption can proceed is reached when  $1.0 > c_{\text{Na}}^m > 0.1$  mm.

Despite the protective value of low junctional permeabilities in very hypoosmotic mucosal media, net Na<sup>+</sup> reabsorption is enhanced by increasing the junctional permeabilities when  $c_{\text{Na}}^m = 120$  mm (column 5 of Table 4). This junctional effect is predicted by all of the simulations performed; the magnitude of the enhancement varies from 14.7 to 18.8%, depending upon the specific model considered (Table 3). Thus, the body's stores of Na<sup>+</sup> are maximally conserved under physiological open-circuited con-

ditions when the junctional permeabilities are responsive to  $\pi^m$ , increasing when  $\pi^m$  and  $c_{\text{Na}}^m$  are high, and decreasing when  $\pi^m$  and  $c_{\text{Na}}^m$  are low, as observed experimentally (Civan & DiBona, 1978).

As noted earlier, the intracellular Na<sup>+</sup> concentration is higher in the short-circuited than in the open-circuited state, when the tissue is bathed with identical Na<sup>+</sup> Ringer's solutions. This effect was consistently noted for all of the mucosal media studied with all of the model simulations. However, its magnitude was strongly dependent upon  $c_{\text{Na}}^m$ . When  $c_{\text{Na}}^m = 120$  mm, the modified model without a Cl-pump predicts  $c_{\text{Na}}^i$  to be reduced by 56.0% by open circuiting the tissue (Table 4); this reduction is only 3.6% when  $c_{\text{Na}}^m = 0.1$  mm.

The relationship between the short-circuit current ( $I_T$ ) and net Na<sup>+</sup> transport  $(I_{\text{Na}})_T$  is also strongly dependent upon  $c_{\text{Na}}^m$  under the conditions of the current simulations. The two parameters are similar when  $c_{\text{Na}}^m = 120$  or 11.5 mm. However, they differ by a factor of about three for  $c_{\text{Na}}^m = 1.0$  mm and assume different signs altogether for  $c_{\text{Na}}^m = 0.1$  mm (Table 4).

The relative importance of recycling of Na<sup>+</sup> across the basolateral membrane is also strongly dependent upon  $c_{\text{Na}}^m$  (Table 2). In the open-circuited state, 21.6% of the net Na<sup>+</sup> entry into the cell proceeds across the basolateral membrane when  $c_{\text{Na}}^m = 120$  mm, while 71.2% occurs at this site when  $c_{\text{Na}}^m = 1.8$  mm. The comparable contributions at the higher and lower mucosal Na<sup>+</sup> concentrations are 9.1% and 49.2%, respectively, in the short-circuited state (Table 2).

## Discussion

The current work has utilized the basic model of Lew et al. (1979), a formulation based largely on the

concepts of Koefoed-Johnsen and Ussing (1958) and incorporating a minimal number of additional widely-held assumptions. The great strengths of the basic model are: (i) its flexibility, free from the constraining assumptions of linearity, (ii) its ability, documented both here and previously (Lew et al., 1979), to generate stable steady-state computations, even under extreme conditions commonly imposed experimentally, and (iii) the unusual opportunity it provides to study transient transport behavior.

As in all current models of transepithelial transport, the most serious limitation of the basic model lies in the uncertainty of how to describe realistically the electrophysiological kinetics of the Na/K-exchange pump at the basolateral membrane. The basic rheogenic model considers the pump to be a current source whose output is independent of the basolateral membrane potential, an approach taken recently by a number of investigators (e.g., Sackin & Boulpaep, 1975; Lindemann, 1979; Gordon, 1981). This concept constitutes a substantive departure from the electrogenic formalism suggested by Koefoed-Johnsen and Ussing (1958) and subsequently adopted by most investigators, in which the pump is described as a voltage source whose driving force is independent of current density. In the absence of compelling evidence identifying one or the other formalism as the more realistic description, it has been useful to apply both formalisms to the same problem.

On the basis of their measurements of radioactive Na<sup>+</sup> flux across toad bladder conducted under short-circuited conditions, and analyzed in terms of a linear electrogenic model, Civan and DiBona (1978) have suggested a physiological role for the apical intercellular junctions in minimizing urinary NaCl loss; a similar conclusion was reached by Reuss and Finn (1975) on the basis of their electrophysiologic data. Civan and DiBona observed that the junctional permeability for Na<sup>+</sup> is reduced by a factor of 1.49 when bladders are bathed with hypoosmotic hyponatric mucosal media, rather than with isoosmotic sodium Ringer's solution. Their calculations suggested that the higher junctional permeability found with isoosmotic mucosal media should increase net NaCl reabsorption under physiologic open-circuited conditions by about 16%. The nonlinear rheogenic simulations of the present study predict increases of 15–19%, depending upon the specific form of the model considered. When the mucosal Na<sup>+</sup> concentration is very low, both models predict that the observed reductions in junctional permeabilities enhance net NaCl reabsorption, or under highly unfavorable circumstances, reduce net NaCl secretion into the urine. The good quantitative agreement between the results generated

by the two fundamentally different approaches strongly supports the concept that the apical tight junctions modulate transepithelial NaCl transport under physiological conditions. It should be appreciated that this role is important only for tight epithelia such as toad bladder and frog skin with low apical permeabilities to Cl<sup>−</sup> (Civan & DiBona, 1978); under these circumstances, the junctional permeability to Cl<sup>−</sup> becomes a rate-limiting factor in NaCl transport under physiologic conditions.

The current study of hypoosmotic mucosal conditions has also documented that net NaCl reabsorption can be simulated by the modified program, even at the lowest values of  $c_{\text{Na}}^m$  physiologically observed (1.8 mM), without involving any ad hoc changes in ionic permeabilities or pump rates (Lew et al., 1979). Models incorporating an apical Cl-pump predict persistent NaCl reabsorption for  $1.0 > c_{\text{Na}}^m > 0.1$  mM. However, for  $c_{\text{Na}}^m \leq 0.1$  mM, net reabsorption can be simulated only if the model parameters are changed, either as suggested by Lew et al. (1979) or by incorporating an additional specialized Na<sup>+</sup> transfer mechanism in the apical membrane.

In studying the effects of reducing mucosal Na<sup>+</sup> concentration, certain striking differences between the short-circuited and open-circuited states have been emphasized. All of the specific forms of the rheogenic model under consideration predicted an approximately 2½-fold reduction in intracellular Na<sup>+</sup> concentration upon open-circuiting the epithelium when  $c_{\text{Na}}^m = 120$  mM. This prediction is contrary to the observed similarity in  $c_{\text{Na}}^c$  measured either chemically (Robinson & Macknight, 1976*b*) or with the electron microprobe (Rick et al., 1978*b*; Civan et al., 1980) under open-circuited and short-circuited conditions. The present simulations predict that in the transition between these two states,  $c_{\text{Na}}^c$  should change by some 20% within a period of 30 sec. The absence of any such measurable difference raises at least two possibilities. The experimental preparative procedure used to transfer the short-circuited preparation to a form suitable for quantitative analysis may have been too slow; thus, the tissues analyzed may have effectively been in the open-circuited state, whether or not the experiment had first been conducted in the short-circuited condition. Alternatively, current concepts concerning the electrodiffusive nature of apical Na<sup>+</sup> entry may be qualitatively or quantitatively incorrect.

Study of hyponatric mucosal solutions has also clarified the relation between net Na<sup>+</sup> transport ( $I_{\text{Na}}$ )<sub>T</sub> and short-circuit current ( $I_T$ ). Models based on the formulation of Koefoed-Johnsen and Ussing (1958) predict closely similar values for the two parameters so long as  $c_{\text{Na}}^m \geq 11.5$  mM. However, sub-

stantial discrepancies are expected for  $c_{\text{Na}}^m \leq 1.0$  mM, even if their classical formulation is correct.

One of the most striking observations of the present study has been that the fractional entry of  $\text{Na}^+$  across the basolateral membrane can be an order of magnitude greater than that across the apical membrane. The precise quantitative predictions are of limited importance, insofar as the values of  $P_{\text{Na}}^{bl}$  under baseline and experimental conditions are yet to be rigorously determined; the value chosen by Lew et al. (1979) and retained here may well prove to be an overestimate. However, the current work documents the qualitative importance of basolateral  $\text{Na}^+$  entry under certain experimental conditions. The simulations of the present study have emphasized that fractional entry of  $\text{Na}^+$  across the basolateral membrane is clearly a function of transepithelial potential, mucosal  $\text{Na}^+$  concentration and serosal  $\text{K}^+$  concentration. Thus, although fractional basolateral entry is clearly modest under baseline short-circuited conditions with  $c_{\text{Na}}^m \simeq 120$  mM and  $c_{\text{K}}^s \geq 2.5$  mM (Sharp & Leaf, 1966; Coplon & Maffly, 1972; Canessa, Labarca & Leaf, 1976; Hong & Essig, 1976; Table 2), it can be unwise to assume that  $P_{\text{Na}}^{bl} = 0$  under other conditions (Hviid Larsen, 1978; Hviid Larsen & Kristensen, 1978). Two-thirds to three-quarters of net electrodiffusive  $\text{Na}^+$  entry is calculated to proceed across the basolateral membrane in the open-circuited state with  $c_{\text{Na}}^m = 1.8$  mM (Table 2). When  $c_{\text{K}}^s$  is lowered to 0.25 mM, the current simulations predict that net basolateral  $\text{Na}^+$  entry will actually become an order of magnitude greater than that across the apical membrane (Fig. 9); the modified model thus helps reconcile the observations that the experimental reduction of  $c_{\text{K}}^s$  markedly increases the total  $c_{\text{Na}}^s$  (Civan et al., 1980) without measurably altering the intracellular  $\text{Na}^+$  contents of mucosal origin (Robinson & Macknight, 1976b).

The application of the current computer model has also been of great value in analyzing other effects of reducing  $c_{\text{K}}^s$ . The data presented clearly demonstrate that the basic model of Lew et al. (1979), with or without a Cl-pump, cannot satisfactorily simulate several experimentally observed effects. These authors were aware of certain limitations of their basic model, and emphasized the role of apical  $\text{Na}^+$  permeability in slowing the rate of loss of cell  $\text{K}^+$  induced by ouabain. In the present study, following reduction of  $c_{\text{K}}^s$ , the basic model could not reproduce: (i) the surprisingly slow rate of elution of intracellular  $\text{K}^+$  (Robinson & Macknight, 1976b; Civan et al., 1980), (ii) the large fall in transepithelial conductance (DeLong & Civan, 1978, 1979), and (iii) the lag time dissociation between cellular  $\text{K}^+$  uptake

and short-circuit current noted following restoration of serosal  $\text{K}^+$  to toad bladder (DeLong & Civan, 1978, 1979). These limitations can be largely repaired, at least qualitatively, by taking account of the negative feedback interaction between  $P_{\text{Na}}^a$  and  $c_{\text{Na}}^s$  suggested by several investigators (Erlj & Smith, 1973; Leblanc & Morel, 1975; Morel & Leblanc, 1975; Lewis et al., 1976; Cuthbert & Shum, 1977; Turnheim et al., 1978; Weinstein et al., 1980). Thus, the current study demonstrates that reducing the serosal  $\text{K}^+$  concentration very likely reduces  $\text{Na}^+$  transport in part by inhibiting apical  $\text{Na}^+$  entry as initially proposed by Essig and Leaf (1963), albeit for different reasons.

This work was supported in part by a research grant from the National Institutes of Health (AM 20632). We are exceedingly grateful to Dr. Virgilio L. Lew for his great help in providing us with technical details concerning the computer programs developed by Lew, Ferreira and Moura (1979), and for apprising us of the variable affinity modification he is currently using and which was adopted here. We are also grateful to Dr. Stephen Baylor for graciously granting us access to his computer facility.

## References

- Biber, T.U.L., Walker, T.C., Mullen, T.L. 1980. Influence of extracellular Cl transport across isolated skin of *Rana pipiens*. *J. Membrane Biol.* **54**:191-202
- Bobrycki, V.A., Mills, J.W., Macknight, A.D.C., DiBona, D.R. 1981. Structural responses to voltage-clamping in the toad urinary bladder: I. The principal role of granular cells in the active transport of sodium. *J. Membrane Biol.* **60**:21-33
- Bond, M., Shporer, M., Peterson, K., Civan, M.M. 1981.  $^{31}\text{P}$  Nuclear magnetic resonance analysis of toad urinary bladder. *Mol. Physiol.* **1**:243-263
- Canessa, M., Labarca, P., Leaf, A. 1976. Metabolic evidence that serosal sodium does not recycle through the active transepithelial transport pathway of toad bladder. *J. Membrane Biol.* **30**:65-77
- Civan, M.M. 1978. Intracellular activities of sodium and potassium. *Am. J. Physiol.* **234**:F261-F269
- Civan, M.M. 1981. Intracellular  $\text{K}^+$  in toad urinary bladder: Results from microelectrode and electron microprobe analyses. In: *Ion Transport By Epithelial Tissues*. S.G. Schultz, editor. pp. 129-136. Raven Press, New York
- Civan, M.M., DiBona, D.R. 1974. Pathways for movement of ions and water across toad urinary bladder. II. Site and mode of action of vasopressin. *J. Membrane Biol.* **19**:195-220
- Civan, M.M., DiBona, D.R. 1978. Pathways for movement of ions and water across toad urinary bladder. III. Physiologic significance of the paracellular pathway. *J. Membrane Biol.* **38**:359-386
- Civan, M.M., Hall, T.A., Gupta, B.L. 1980. Microprobe study of toad urinary bladder in absence of serosal  $\text{K}^+$ . *J. Membrane Biol.* **55**:187-202
- Coplon, N.S., Maffly, R.H. 1972. The effect of ouabain on sodium transport and metabolism of the toad bladder. *Biochim. Biophys. Acta* **282**:250-254
- Cuthbert, A.W., Shum, W.K. 1977. Does intracellular sodium



- modify membrane permeability to sodium ions? *Nature (London)* **266**:468-469
- Davies, H.E.F., Martin, D.G., Sharp, G.W.G. 1968. Differences in the physiological characteristics of bladders from different geographical sources. *Biochim. Biophys. Acta* **150**:315-318
- DeLong, J., Civan, M.M. 1978. Dissociation of cellular K<sup>+</sup> accumulation from net Na<sup>+</sup> transport by toad urinary bladder. *J. Membrane Biol.* **42**:19-43
- DeLong, J., Civan, M.M. 1979. Intracellular potassium activity associated with potassium depletion from toad urinary bladder. *Colloq. Inst. Nat. Santé Rech. Med.* **85**:221-229
- DiBona, D.R., Civan, M.M. 1973. Pathways for movement of ions and water across toad urinary bladder: I. Anatomic site of transepithelial shunt pathways. *J. Membrane Biol.* **12**:101-128
- Duffey, M.E., Thompson, S.M., Frizzell, R.A., Schultz, S.G. 1979. Intracellular chloride activities and active chloride absorption in the intestinal epithelium of the winter flounder. *J. Membrane Biol.* **50**:331-341
- Duffey, M.E., Turnheim, K., Frizzell, R.A., Schultz, S.G. 1978. Intracellular chloride activities in rabbit gallbladder: Direct evidence for the role of the sodium-gradient in energizing "uphill" chloride transport. *J. Membrane Biol.* **42**:229-245
- Erecińska, M., Wilson, D.F., Nishiki, K. 1978. Homeostatic regulation of cellular energy metabolism: Experimental characterization *in vivo* and fit to a model. *Am. J. Physiol.* **234**:C82-C89
- Erlj, D., Smith, M.W. 1973. Sodium uptake by frog skin and its modification by inhibitors of transepithelial sodium transport. *J. Physiol (London)* **228**:221-239
- Essig, A. 1965. Active sodium transport in toad bladder despite removal of serosal potassium. *Am. J. Physiol.* **208**:401-406
- Essig, A., Caplan, S.R. 1979. The use of linear nonequilibrium thermodynamics in the study of renal physiology. *Am. J. Physiol.* **236**:F211-F219
- Essig, A., Caplan, S.R. 1981. Active transport: Conditions for linearity and symmetry far from equilibrium. *Proc. Natl. Acad. Sci. USA* **78**:1647-1651
- Essig, A., Leaf, A. 1963. The role of potassium in active transport of sodium by the toad bladder. *J. Gen. Physiol.* **46**:505-515
- Finkelstein, A., Mauro, A. 1963. Equivalent circuits as related to ionic systems. *Biophys. J.* **3**:215-237
- Finn, A.L., Handler, J.S., Orloff, J. 1967. Active chloride transport in the isolated toad bladder. *Am. J. Physiol.* **213**:179-184
- Frizzell, R., Field, M., Schultz, S.G. 1979. Sodium-coupled chloride transport by epithelial tissues. *Am. J. Physiol* **236**:F1-F8
- Frömter, E., Gebler, B. 1977. Electrical properties of amphibian urinary bladder epithelia. III. The cell membrane resistances and the effect of amiloride. *Pfluegers Arch.* **371**:99-108
- Fuchs, W., Hviid Larsen, E., Lindemann, B. 1977. Current-voltage curve of sodium channels and concentration dependence of sodium permeability in frog skin. *J. Physiol. (London)* **267**:137-166
- Garay, R.P., Garrahan, P.J. 1973. The interaction of sodium and potassium with the sodium pump in red cells. *J. Physiol. (London)* **231**:297-325
- Goldman, D.E. 1943. Potential, impedance and rectification in membranes. *J. Gen. Physiol.* **23**:37-60
- Gordon, L.G.M. 1981. Electrochemical properties of toad urinary bladder. In: Epithelial Ion and Water Transport. A.D.C. MacKnight and J. Leader, editors. pp. 297-306. Raven Press, New York
- Grinstein, S., Erlj, D. 1978. Intracellular calcium and the regulation of sodium transport in the frog skin. *Proc. R. Soc. London B* **202**:353-360
- Gupta, B.L., Hall, T.A. 1979. Quantitative electron probe X-ray microanalysis of electrolyte elements within epithelial tissue compartments. *Fed. Proc.* **38**:144-153
- Glynn, I.M., Karlsh, S.J.D. 1975. The sodium pump. *Annu. Rev. Physiol.* **37**:13-55
- Guynn, R.W., Veech, R.L. 1973. The equilibrium constants of the adenosine triphosphate hydrolysis and the adenosine triphosphate-citrate lyase reactions. *J. Biol. Chem.* **248**:6966-6972
- Handler, J.S., Preston, A.S., Orloff, J. 1969. The effect of aldosterone on glycolysis in the urinary bladder of the toad. *J. Biol. Chem.* **244**:3194-3199
- Helman, S.I., Fisher, R.S. 1977. Microelectrode studies of the active Na transport pathway of frog skin. *J. Gen. Physiol.* **69**:571-604
- Helman, S.I., Miller, D.A. 1974. Edge damage effect on measurements of urea and sodium flux in frog skin. *Am. J. Physiol.* **226**:1198-1208
- Helman, S.I., Nagel, W., Fisher, R.S. 1979. Effects of ouabain on active transepithelial sodium transport in frog skin: Studies with microelectrodes. *J. Gen. Physiol.* **74**:105-127
- Hodgkin, A.L., Huxley, A.F. 1952. A quantitative description of membrane current and its application to conduction and excitation in nerve. *J. Physiol. (London)* **117**:500-544
- Hodgkin, A.L., Katz, B. 1949. The effect of sodium ions on the electrical activity of the giant axon of the squid. *J. Physiol (London)* **108**:37-77
- Hoffman, J., Tosteson, D.C. 1971. Active sodium and potassium transport in high potassium and low potassium sheep red cells. *J. Gen. Physiol.* **58**:438-466
- Hong, C.D., Essig, A. 1976. Effects of 2-deoxy-D-glucose, amiloride, vasopressin, and ouabain on active conductance and  $E_{Na}$  in the toad bladder. *J. Membrane Biol.* **28**:121-142
- Hviid Larsen, E. 1978. Computed steady-state ion concentrations and volume of epithelial cells. Dependence on transcellular Na<sup>+</sup> transport. Alfred Benzon Symposium **XI**:438-456. Munksgaard, Copenhagen
- Hviid Larsen, E., Kristensen, P. 1978. Properties of a conductive cellular chloride pathway in the skin of the toad (*Bufo bufo*). *Acta Physiol. Scand.* **102**:1-21
- Katchalsky, A., Curran, P.F. 1967. Nonequilibrium Thermodynamics in Biophysics. 248 pp. Harvard University Press, Cambridge, Mass.
- Kimura, G., Spring, K.R. 1978. Transcellular and paracellular tracer chloride fluxes in *Necturus* proximal tubule. *Am. J. Physiol.* **235**:F617-F625
- Klingenberg, M. 1968. The respiratory chain: In: Biological Oxidations. T.P. Singer, editor. pp. 3-54. Wiley, New York
- Koefoed-Johnsen, V., Ussing, H.H. 1958. The nature of the frog skin potential. *Acta Physiol. Scand.* **42**:298-308
- Leaf, A. 1965. Transepithelial transport and its hormonal control in toad bladder. *Ergeb. Physiol. Biol. Chem. Exp. Pharmacol.* **56**:216-263
- Leaf, A., Anderson, J., Page, L.B. 1958. Active sodium transport by the isolated toad bladder. *J. Gen. Physiol.* **41**:657-668
- Leblanc, G., Morel, F. 1975. Na and K movements across the membranes of frog skin associated with transient current changes. *Pfluegers Arch.* **358**:159-177
- Lew, V.L., Ferreira, H.G., Moura, T. 1979. The behaviour of transporting epithelial cells: I. Computer analysis of a basic model. *Proc. R. Soc. London B* **206**:53-83
- Lewis, S.A., Eaton, D.C., Diamond, J.M. 1976. The mechanism of Na<sup>+</sup> transport by rabbit urinary bladder. *J. Membrane Biol.* **28**:41-70
- Lindemann, B. 1979. The minimal information content of  $E_{Na}$ . *Colloq. Inst. Natl. Santé Rech. Med.* **85**:241-252
- Lindemann, B. 1980. The beginning of fluctuation analysis of epithelial ion transport. *J. Membrane Biol.* **54**:1-11
- Macchia, D.D., Helman, S.I. 1976. Anion permeability of non-edge damaged frog skin. *Biophys. J.* **16**:131a
- Macknight, A.D.C., Civan, M.M., Leaf, A. 1975a. The sodium

- transport pool in toad urinary bladder epithelial cells. *J. Membrane Biol.* **20**:365–386
- Macknight, A.D.C., Civan, M.M., Leaf, A. 1975*b*. Some effects of ouabain on cellular ions and water in epithelial cells of toad urinary bladder. *J. Membrane Biol.* **20**:387–401
- Macknight, A.D.C., DiBona, D.R., Leaf, A., Civan, M.M. 1971. Measurement of the composition of epithelial cells from the toad urinary bladder. *J. Membrane Biol.* **6**:108–126
- Mandell, L.J., Curran, P.F. 1972. Response of the frog skin to steady-state voltage clamping: I. The shunt pathway. *J. Gen. Physiol.* **59**:503–518
- Morel, F., Leblanc, G. 1975. Transient current changes and Na compartmentalization in frog skin epithelium. *Pfluegers Arch.* **358**:135–157
- Nagel, W. 1976. The intracellular electrical profile of the frog skin epithelium. *Pfluegers Arch.* **365**:135–143
- Nagel, W. 1980. Rheogenic sodium transport in a tight epithelium, the amphibian skin. *J. Physiol. (London)* **302**:281–295
- Nagel, W., Garcia-Diaz, J.F., Armstrong, W.McD. Intracellular ionic activities in frog skin. *J. Membrane Biol. (in press)*
- Nagel, W., Pope, M.B., Peterson, K., Civan, M.M. 1980. Electrophysiologic changes associated with potassium depletion of frog skin. *J. Membrane Biol.* **57**:235–241
- Reuss, L., Finn, A.L. 1975. Effects of changes in the composition of the mucosal solution on the electrical properties of the toad urinary bladder epithelium. *J. Membrane Biol.* **20**:191–204
- Reuss, L., Grady, T.P. 1979. Effects of external sodium and cell membrane potential on intracellular chloride activity in gallbladder epithelium. *J. Membrane Biol.* **51**:15–31
- Rick, R., Dörge, A., Arnim, E. von, Thureau, K. 1978*a*. Electron microprobe analysis of frog skin epithelium: Evidence for a syncytial Na transport compartment. *J. Membrane Biol.* **39**:313–331
- Rick, R., Dörge, A., Macknight, A.D.C., Leaf, A., Thureau, K. 1978*b*. Electron microprobe analysis of the different epithelial cells of toad urinary bladder. *J. Membrane Biol.* **39**:257–271
- Robinson, B.A., Macknight, A.D.C. 1976*a*. Relationships between serosal medium potassium concentration and sodium transport in toad urinary bladder: I. Effects of different medium potassium concentrations on electrical parameters. *J. Membrane Biol.* **26**:217–238
- Robinson, B.A., Macknight, A.D.C. 1976*b*. Relationships between serosal medium potassium concentration and sodium transport in toad urinary bladder: II. Effects of different medium potassium concentrations on epithelial cell composition. *J. Membrane Biol.* **26**:239–268
- Rothschild, K.J., Elias, S.A., Essig, A., Stanley, H.E. 1980. Non-equilibrium linear behavior of biological systems: Existence of enzyme-mediated multidimensional inflection points. *Biophys. J.* **30**:209–230
- Sackin, H., Boulpaep, E.L. 1975. Models for coupling of salt and water transport. Proximal tubular reabsorption in *Necturus* kidney. *J. Gen. Physiol.* **66**:671–734
- Saito, T., Lief, P.D., Essig, A. 1974. Conductance of active and passive pathways in the toad bladder. *Am. J. Physiol.* **226**:1265–1271
- Sawyer, W.H. 1956. The antidiuretic action of neurohypophyseal hormones in Amphibia. *Proc. Symp. Colston Res. Soc.* **8**:171–182
- Sharp, G.W.G., Leaf, A. 1966. Mechanism of action of aldosterone. *Physiol. Rev.* **46**:593–633
- Slater, E.C. 1969. The oxidative phosphorylation potential. In: *The Energy Level and Metabolic Control in Mitochondria*. S. Papa, J.M. Tager, E. Qualiarrello, and E.C. Slater, editors. pp. 225–259. Adriatica Editrice, Bari
- Taylor, A., Windhager, E.E. 1979. Possible role of cytosolic calcium and Na–Ca exchange in regulation of transepithelial sodium transport. *Am. J. Physiol.* **236**:F505–F512
- Thomas, S.R., Mikulecky, D. 1978. A network thermodynamic model of salt and water flow across the kidney proximal tubule. *Am. J. Physiol.* **235**:F638–F648
- Turnheim, K., Frizell, R.A., Schultz, S.G. 1978. Interaction between cell sodium and amiloride-sensitive sodium entry in rabbit colon. *J. Membrane Biol.* **39**:233–256
- Ussing, H.H. 1960. *The Alkali Metal Cations in Biology*. H.H. Ussing, P. Kruhoffer, J.H. Thaysen, and N.A. Thorn, editors. 195 pp. Springer-Verlag, Berlin-Heidelberg-Göttingen
- Ussing, H.H. 1965. Relationship between osmotic reactions and active sodium transport in the frog skin epithelium. *Acta Physiol. Scand.* **63**:141–155
- Ussing, H.H., Zerahn, K. 1951. Active transport of sodium as the source of electric current in the short-circuited isolated frog skin. *Acta Physiol. Scand.* **23**:110–127
- Voûte, C.L., Ussing, H.H. 1968. Some morphological aspects of active sodium transport. The epithelium of the frog skin. *J. Cell. Biol.* **36**:625–638
- Walser, M. 1970. Role of edge damage in sodium permeability in toad bladder and a means of avoiding it. *Am. J. Physiol.* **219**:252–255
- Weinstein, F.C., Rosowski, J.J., Peterson, K., Delalic, Z., Civan, M.M. 1980. Relationship of transient electrical properties to active sodium transport by toad urinary bladder. *J. Membrane Biol.* **52**:25–35

Received 24 April 1981; revised 16 July 1981